We thank all reviewers for valuable comments and suggestions. After considering them, we see that the quality of the manuscript has improved. Work is planned on further development of the retrieval algorithm based on the validation results reported in the manuscript. Some of the comments/suggestions will be considered during the evaluation of the next version of the Sy AOD product.

Response to anonymous reviewer #1

We thank the reviewer for her/his very helpful suggestions

RC1: 'Sogacheva et al. (2022) amt-2022-101', Anonymous Referee #2, 03 Jun 2022 reply

Review for Atmospheric Measurement Techniques

Title: Extended validation and evaluation of the OLCI-SLSTR Synergy aerosol product (SY_2_AOD) on Sentinel-3

Authors: Larisa Sogacheva, Matthieu Denisselle, Pekka Kolmonen, Timo H. Virtanen, Peter North, Claire Henocq, Silvia Scifoni and Steffen Dransfeld

General Comments:

This manuscript presents a very thorough and detailed validation of the SY_2_AOD and related Angstrom Exponent products by comparison to AERONET and MODIS data sets. This analysis provides the user community with the statistics that are required to intelligently utilize these datasets. What is somewhat lacking in many sections (see some specifics below) are explanations and/or reasons for poor performance in the satellite retrieval AOD products versus AERONET measured AOD in some specific regions. This contrasts with much better performance in other regions yet there is little to no discussion on why some regions are much better than others.

There are common reasons why the performance of retrieval algorithms is worse at certain conditions (e.g., cloud and snow contamination), in specific regions (e.g., bright surface), and for specific instrument-related reasons (e.g., influence of the viewing geometry, as for S3). Those reasons are mentioned in the text (e.g., lines 154, 205, 865 as in AMTD)

I think the authors should include much more discussion on the likely algorithmic and/or physical reasons for the discrepancies in the problem regions, much as they did in the last paragraph of the Conclusions section.

As suggested by all three reviewers, more discussion on the likely algorithmic and/or physical reasons for the discrepancies between Sy_2 and reference products was included.

Additionally I feel that this paper is too long with too many multi-panel figures for most readers. I suggest that the authors select a significant fraction of the figures (maybe one third) and associated text and move them to an appendix section. This would significantly improve the readability and clarity of the paper.

One figure and five tables are moved to the Supplement

Specific Comments:

***Lines 28-30**, Abstract: “The retrieval of Angstrom exponent, related to aerosol size distribution, shows good spatial correlation with expected sources but generally overestimates AE for cases where AERONET Angstrom is low, resulting in overall high bias.” I think this somewhat overstates the accuracy and utility of the satellite retrieved AE. The regional AE comparisons in Figure 24 show very poor accuracy for most regions in the satellite AE product. I suggest removing this sentence from the abstract or making a more quantitative statement on the retrieved AE accuracy.*

The statement on the AE is re-formulated.

Similar comments can be applied to the poor retrieval accuracy of the satellite FMF in Figure 22, except for good agreement at the highest AOD levels.

Conclusions on the FMF and FMAOD are added to the abstract

***Line 172-173**: Please describe somewhere in the text how is AE computed from FMF.*

The section 2.2.3 is now clarified: "During post-processing, further aerosol outputs are derived from the retrieved AOD_{550} and FM AOD. This includes spectral variation of AOD, which is given using pre-computed look-up table from the retrieved FM AOD and aerosol mixture. The Angstrom exponent is computed based on a pair of spectral AOD values. Here we choose 865nm and 550nm."

***Line 176**: Typo, I assume 'duct' is supposed to be 'dust'.*

The typo is corrected

***Line 196-197**: Please provide a brief explanation as to why the back scatter at the TOA is more critical in the northern hemispheres versus the southern. Is this just because the percentage of land in the SH is much lower? This is an example of a general lack of physical/algorithm explanations for anomalies and/or comparison results in this manuscript.*

The text for this at line 181 has been rewritten: "In the NH, the SLSTR oblique scan generally samples backscattered radiance, which has a weaker aerosol contribution than the corresponding forward scattering sampled in the SH (e.g., https://www-cdn.eumetsat.int/files/2021-09/SARP_Report_Option_1_final.pdf). This leads to reduced quality in AOD in the Northern Hemisphere (NH) compared with Southern Hemisphere (SH) for the SLSTR products, which has been revealed earlier (https://climate.esa.int/media/documents/Aerosol_cci_PVIR_v1.2_final.pdf). For this reason, SY_2 AOD products from the NH and SH were validated separately."

***Line 250**: 'was be' should be 'has been'*

corrected

***Line 265-266**: It might be noted that the MAN instruments are calibrated against the same reference instruments as utilized in AERONET. These reference instruments are calibrated by Langley method at Mauna Loa Observatory to an accuracy of 0.002 to 0.005 in the visible and near IR and ~0.009 in the UV.*

The sentence is added, as suggested

***Line 287**, Section 6.1: Since AERONET does not measure at 550 nm, please note the spectral interpolation method used. Note that the quadratic or 2nd order fit of AOD versus wavelength is more accurate than the linear or Angstrom fit.*

AE fit was used for interpolation; clarification is added

***Line 295-296**: It seems the word 'error' or 'bias' may be missing here. How could 91% of AOD be < 0.04? This AOD level is too low for the majority of the earth.*

The typo (0.04) is corrected to 0.4

***Line 311**: Please define the acronym GCOS here.*

GCOS acronym is added

***Line 380**: Please provide some reasons or explanation for the smaller retrieval errors in the SH.*

This has been now summarised at line 196 (see earlier comment).

***Line 396-397**: An obvious missing region is the Pacific Ocean since oceans dominate the Earth's surface (70%). The Arctic Ocean, Indian Ocean, Southern Ocean, are also very important. Why were these regions not included?*

Validation was performed over Pacific and Indian islands where AERONET stations are located. However, the number of the matchups is critically low over those ocean regions to provide solid conclusion.

***Line 408**: It is surprising that the performance is poor for Europe. An explanation of the reason is warranted here.*

For these three comments (408, 409, 414) we feel the correct place to address these discussing is in the conclusion/discussion section, which has now been extended and addresses these points.

***Line 409**: The scatter and results for the boreal forest region are very poor. This is surprising since the surface is dark (green forests) and the aerosol type is dominated by fine mode (biomass burning smoke). Please explain/discuss the causes of the poor accuracy retrievals in this region.*

This comment is answered above

Line 414: *An explanation is certainly needed/expected for the large regional differences in the fraction of pixels in EE.*

This comment is answered above

***Line 417-419**: The Aus and AOb regions both had very low AOD, none>0.3 so that is a major factor. This should be mentioned in the text otherwise it is somewhat misleading to the reader.*

Details suggested are added to the text

Lines 444-448, *Section 6.1.4: This is an awkward writing style to have a section consist of mainly one line equations and short statements, with no full sentences. I suggest trying to expand it a little to make more readable.*

Section 6.1.4 includes three sub-sections. In the introduction to this section (lines 444-448) we provide only a definition of the relative offset, which is analysed and discussed with respect to different variables (latitude, surface reflectance, ets.) in sub-sections 6.1.4.1-6.1.4.3.

Line 467-468: *In Figure 9 I am missing the separation of NH and SH data that you suggest here. Is there a missing label or legend in this figure?*

There was a typo in the text. The analysis was performed not for the globe, NH and SH, but for dual, singleN and singleO matchups. The sentence was revised

Line 521-523: *The AOD decreases significantly as wavelength increases (except for dust). This may be part of the reason for the offset and rms to decrease as wavelength increases.*

Clarification is added to the text

There is almost consistently a lack of explanation for the observations/comparisons in this manuscript.

The main goal of this work (performed in the frame of ESA LAW project) was to evaluate SY_2 AOD product, reveal problems in the retrieval algorithm and notify algorithm developer and potential users about algorithm performance and product quality in different conditions. We also showed that quality is different for different approaches (e.g, dual or single). In case reasons for limited quality were clear (e.g., back scattering contribution, cloud/snow contamination, bright surface), they are mentioned in the text. However, often a throw revision of the retrieval algorithm is needed to find a reason for a limited performance. This work is planned.

Line 642-643: *This is too vague, it does not really say how the AERONET fine mode AOD from SDA was estimated at 550 nm from the 500 nm product. Please provide more detail here.*

A link for the $aAOD_{500}$ to $aAOD_{550}$ conversion is provided

Line 733-734: *A bias in AE of ~1 and rms of 0.5 effectively renders the satellite retrieval of AE as almost useless for most applications. This should be discussed or summarized in the text.*

The AE in table 7 (which is now moved to the supplement) shows consistent positive correlation with AERONET values, albeit with low R values. We see similar patterns in the retrieval of FMF by MODIS as with SLSTR (new Fig. 28), and SLSTR uniquely gives continuous retrieval over land.

Line 735: *By what metric is this syAE considered 'good' quality? I cannot agree with your assessment unless you define 'good' more clearly.*

We move the description of these as 'good', and more simply report the performance.

Line 740: *Validation over ocean: Why are the AE retrievals not compared for over ocean? This would be a useful comparison/validation to include.*

MAN AE (mAE) is provided for 440-870 nm only; Direct comparison between mAE and syAE is not possible

Line 793-794: *Any ideas or explanation about this large difference between MODIS and Sentinel S3A retrievals over Nigeria? This is a striking gradient in large AOD differences, both positive and negative. Which one is more likely to be closer to reality? This is another example of the lack of analysis in giving some explanations in this paper.*

A reason for the large difference is still unclear. We looked at syFMF and modFMF products (new Fig. 27 in the revised version), but modFMF (provided in MOD04_L2 product) is often missing over land. The reason for the luck of explanation is mentioned above (after comment to line 521-523)

Line 815-816: *The way this sentence is written is confusing and does not make too much sense. Please rephrase and clarify.*

The sentence is rephrased

Line 884-889: *This type of analysis and reasons for biases and differences, while good, are mostly lacking in the main text of this paper. It is strange to wait until the Conclusions section to provide this type of analysis.*

We expanded discussion on the reasons for biases and other differences, where reasons for those were clear. To explain some biases, a through revision of the retrieval algorithm is needed.

Response to anonymous reviewer #2

Thank you very much for your positive review and your helpful comments – they have improved the manuscript greatly.

Review of "Extended validation and evaluation of the OLCI-SLSTR Synergy aerosol product (SY_2_AOD) on Sentinel-3" by Sogacheva et al.

Summary:

This paper presents the synergy AOD product from Sentinel-3 and its evaluation against a set of other global AOD products. This is obviously product of a thorough comparison, from the use of validations against AERONET, MAN (and SURFRAD and SKYNET in supplement), and MODIS datasets, and the breadth and level of detail of the manuscript shows it. This is a high-quality manuscript and should be published in AMT, and will likely be used as reference for many other validation of satellite aerosol products. While this manuscript is long, it is obviously needed, and the quality of the work is appreciated.

I recommend this paper to be published, but after addressing these issues:

- *The linear fitting scheme is not well identified, or may not be appropriate for AOD fitting, and by the manuscript's own analysis (section 6.1.5), this matters for quantifying the overall fit. See the general comment #6. This would not be brought up as major concern except for the fact that it is highlighted in the manuscript already.*

Clarification is added to the text that Pearson correlation coefficient was calculated; linear fitting was performed using polynomial. To shorten the manuscript, as requested by the reviewers, we moved results from Sect. 6.1.5 into the Supplement. Link to the Matlab tool for linear fitting considering uncertainties is provided

- *There are numerous errors in formatting throughout the manuscript which detracts from the quality.*

We checked thoroughly AMT requirements for formats and corrected formats accordingly

- *The description of the retrieval methodology is unclear. How does the retrieval of AOD at multiple wavelength and single scattering albedo is achieved through fitting of AOD at only wavelength (550 nm)?*

This is now clarified (line155): We fit both AOD and FMF, which controls the spectral variation of AOD. All wavelengths of SLSTR, and additionally the 442.5nm OLCI channel over land are used in this fitting.

General Comments:

1. *Several language issues are found within the abstract, and there is need for more quantitative indication in the abstract instead of the subjective descriptions (see specific comments below)*
   We revised the abstract and provided quantitative indication for the results reported
2. *Throughout the document the date format does not seem to meet the AMT standard of "Date and time: 25 July 2007 (dd month yyyy), 15:17:02 (hh:mm:ss)", particularly evident in the paragraph at line 79-89. See the guidelines: https://www.atmospheric-measurementhttps://www.atmospheric-measurement-techniques.net/submission.html - mathtechniques.net/submission.html#math*
   Date format is corrected in the manuscript according to the AMT standard
3. *How much time is passed between measurements in the oblique and nadir view? And how does that impact the aerosol retrieval, particularly near clouds?*

To our knowledge, an offset between oblique and nadir view measurements is 1-2 minutes. Cloud screening is performed for both views; cloud edge test is applied

4. *The retrieval dictates the retrieval of AOD and its fine mode at 550 nm, however returns many more parameters, including single scattering albedo, at various wavelengths. This is poorly described, and is both referred to as 'aerosol properties retrieved' and 'intended as diagnostics' (section 2.2.2). Please clarify what these properties are, and how they are retrieved, especially when only fitting to AOD and fine mode AOD at 550 nm.*

This comment is addressed in Sect. 2.2.2

5. *Many references and citations are only links to websites, many of which should be replaced by the appropriate citation, and many are missing the date accessed.*

Most of the links are for technical specifications of the instruments; these links are suggested by ESA as a reference. We checked citations and changed links to the appropriate citations, where possible. However, since S3 is a relatively new mission, not many results are published in the journals. Thus, we refer to the mission documents and results obtained from other projects which are not published yet. If missing, the dates of acceptance are added.

6. *The type of linear regression is not identified, and this matters for AOD comparisons. Reference to a 'linear regression' between the aAOD and syAOD is presented, however it seems to imply the use of the Ordinary-Least-Squares (OLS) commonly-used fitting routine. This is unlikely to be suitable for this data as the 'independent' variable (aAOD) is subject to uncertainties, and AOD typically do not have gaussian error profiles, which are needed for the OLS. Other fitting routines are recommended to be used, like the 'Yorkfit' (York et al., 2004) or a bivariate regression (e.g., Shinozuka et al., 2015). Similarly, some considerations to the "R" parameter should be mentioned – is it the common Pearson linear correlation coefficient or the Spearman's rank correlation as suggested for use in Sayer et al., 2018. It seems uncertain what is used in Matlab's linear model, or how uncertainty is weighted.*

Clarifications for correlation coefficient and linear regression type are added. We agree that linear regression applied to the full range of AOD does describe details and results may be strongly influences by the outliers. Thus, we included in the revised version binned AOD analysis, which shows AOD offset at different AOD ranges.

7. *There seems to be a significant reduction in error statistics when using the Single Oblique angle, than the single nadir view and even the dual views, however this is not mentioned much, and leads the reader to question the validity of the nadir viewing measurements as a result. (see table 1)*

Pixels retrieved with single processor applied to the oblique view are ocean pixels. Retrieved AOD over ocean is, in general, of better quality, because ocean surface reflectance model provides better results that land reflectance approach.

8. *There seems to be lower discrepancy between syAOD and aAOD in regions of significant biomass burning aerosol (higher AOD Bor, NAW, AOb for example). This raises the question on what type of single scattering albedo is used, and how does the selection of this model impact the AOD retrievals.*

This is now clarified (line 157): The SSA is constrained by climatology for the coarse and fine mode extremes separately and as a priori information. The retrieval of FMF results in a SSA by interpolation between these extremes; however, this should be seen as a potential diagnostic for retrieval performance rather than a user product.

9. *Throughout the conclusions section there is a significant amount of qualitative wording such as 'agreement is good' This is subjective and not always supported by the comparisons presented in this manuscript. Either give comparison values to what it is expected to be, or refrain from these subjective statements.*

Statements like 'agreement is good' are accomplished now with values or removed

10. *There is no mention of potential impact of varying single scattering albedo on the AOD retrieval in the conclusion. Is this a solved issue?*

This is included in the conclusion now.

Specific Comments:

11. *Title: 'Extended' seems to be slightly overexaggerating for a year and half in terms of satellite data comparisons. Suggest to remove that word from the title.*

    We use "extended" not regarding the length of the product, but different validation approaches (including spatial and temporal variations and investigation of the validation results with respect to satellite and solar geometries) and number of variables which are validated and evaluated (AOD, AODunc, FMAOD, FMF, AE)
12. *Line 14: The word 'synergy/synergistic' is used twice in the first sentence.*

    In the first sentence we explain the origin of the name of the product: the name "synergy" comes from the "synergetic" approach. Thus, the word 'synergy/synergistic' is used twice
13. *Line 24: The use of double +/- is confusing, is this the error of the error based on AOD, or the potential range of the error?*

    The error depends on AOD: for higher AOD, the error envelope is wider
14. *Line 29: Use of "Angström" should be consistent throughout the manuscript, the "ö" is missing on this line.*

    Corrected in the whole manuscript
15. *Line 30: AE is not defined.*

    AE is now defined in the previous line
16. *Line 28-35: use of subjective descriptions should be made more quantitative e.g., "good correlation", "agreement is better", "often slightly better". By how much, how often, and compared to what?*

    Quantitative description (when possible) is added
17. *Abstract: the extent of the evaluation is not introduced. How many days, years, or number of comparison points are used here?*

    Validation period is added to the abstract. Since number of the matchups differs from one exercise to another, depending on the tasks, further datails (e.g., number of validation points) are reported in the main text
18. *Line 108, and throughout the manuscript: there should be a space between the number and the unit '500m'*

    Corrected
19. *Line 102 and 105, please reference the proper citations for SENTINEL-3 OLCI and SLSTR instead of the websites.*

    We used citations recommended by ESA
20. *Line 102 and subsequent, is it capital case SENTINEL-3, Sentinel-3, Sentinel 3? Please select one and use is consistently throughout the manuscript.*

    Checked and corrected in the whole manuscript
21. *Line 113, is there a better reference than this website document for the aerosol retrieval? Seems like this is an important publication for better understanding the material presented in this manuscript. Particularly to support the statement "is of variable quality, with higher uncertainty in retreievals in the oblique backscattering direction." (which has a typo at line 114).*

    The manuscript which describes the retrieval is under preparation. Typo is corrected
22. *Does the shift vectors (section 2.2.1) also have a rotational portion, or is it only translational shifts?*

    Small window (grid) moved around the search window (along shift vectors) in OLCI channel geometry (https://sentinels.copernicus.eu/web/sentinel/user-guides/sentinel-3-synergy/definitions/notations)
23. *Lines 137 and 145 seem to be repeated "at least 50% of valid pixels"*

The text is re-phrased, repetition is removed.

24. *Line 147, it is unclear what is meant by 'direction'. Is it viewing direction or viewing angle?*
Viewing direction, clarified in the text
25. *Line 151, Does 442.5 spectral band refer to 442.5 nm ?*
Yes, clarification is provided
26. *Line 186, What is "Copernicus C3S_Lot2" ?*
We added clarification for the project title, but could not find a proper link to the project description and project documents
27. *Line 214, why the shift in multiplication symbol from "x" to "*"?*
"*" is replaced with "x" in the whole manuscript
28. *Figure 2 is too small.*
The fonts are corrected
29. *Line 297, How big are the bins in Figure 2?*
Clarification is added to the figure caption
30. *Line 311, GCOS is not defined.*
GCOS is now defined
31. *Table 1 – decimal point is comma "," instead of point "."*
Done
32. *Line 342, typo "bind"*
Corrected
33. *Line 380, sentence is unclear, is syAOD550 different to S3B $syAOD_{550}$?*
The sentence is re-phrased
34. *Line 446, equation 1 does not seem well formatted*
Equation 1 is now formatted
35. *Line 448, use of * instead of multiplication symbol (×)*
Corrected. Space between x and aAOD is added, because xaAOD is confusing
36. *Line 452, Latitude in [-30 -20] is not well defined, are these degrees south? Is the range inclusive?*
°S is used now instead of '-'
37. *Line 453-457, formatting error? dAODrel or is it $dAOD_{rel}$ or dAOD,rel (in figure 8, 9)*
In the text, formatting is corrected as it is in figures
38. *Line 453, typo? What is "ca"*
Replaced with ~
39. *Figure 8, Units on x-axis not identified (Degrees?)*
Clarification added to the figure caption
40. *Line 547, What is Aerosol_cci+?*
Link to the project is provided in Sect.2.2
41. *Line 595, these distribution don't look very Gauss-like, they seem clearly skewed, particularly singleN.*
Agree, but it is expected to be Gauss-like
42. *Line 617, second apostrophe is not the right side.*
Corrected

43. *Line 672-673, portion of this sentence is in red.*

Corrected

44. *Figure 22, AOd region is missing a portion of the red dashed curve. (similarly in Figure S10 AsN, and S11 AOb)*

Red-dushed curve is missing in the bins where fine-dominated matchups are missing (blue dots, which are results for fine-dominated matchups are also missing then). However, during the checks, we noticed that the fraction of fine-dominated matchups was calculated from the sum of fine- and coarse- dominated, which is right for AOD binned analysis, but not for FMAOD and FMF analysis, where back-ground matchups may exist in any bin. This is corrected, fraction of coarse-dominated is added. Dushed lines for fine- and coarse-dominated fractions are now in blue and green, respectively, as colors for corresponding offsets. The reason for missing a dashed line values at certain bins is the same as it was early – missing fine- or coarse-dominated matchups in the corresponding bin.

45. *Line 698, Isn't AERONET reported at 440 -870 nm? What is a personal estimation? AE difference when using a difference in wavelength has been reported in multiple other papers, e.g., LeBlanc et al., 2020, Yoon et al., 2012*

syAE is reported at 550-870 nm. For evaluation, aAE 500-870 was utilized.

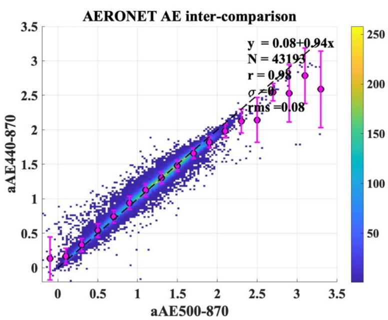

We checked an agreement between $aAE_{440-870}$ and $aAE_{500-870}$ (figure above) and assumed the same agreement between $aAE_{500-870}$ and $aAE_{550-870}$. An offset between $aAE_{440-870}$ and $aAE_{500-870}$ for low (<0.25) AE and high (~2, which is a default value for syAE) AE (which is ~0.2 and ~0.1, respectively) is considerably smaller than an offset between syAE and aAE in those AE size ranges, thus the difference between aAE440-870 and aAE500-870 can be omitted.

46. *Figure 24, There seems to be a common clustering of high syAE, at or just above 2.0. Is this a default limit of AE from the retrieval? Or is this a real behavior of the aerosol?*

This is a default limit of AE from the retrieval

47. *Line 735, "good quality" is subjective, but an rms of greater than 0.5, and R often lower than 0.5, with biases often exceeding 1.0 does not seem to be of 'good quality'.*

We made clarification in the text

48. Table 7, the decimal notation is a comma "," not a dot "."

Corrected

49. *Figure 28, labels of map regions is too small and of bad quality to read.*

Fonts/labels are corrected

50. *Line 785, second time AOI is defined.*

Regions for validation with AERONET are defined in Fig.5, Sect.6.3.1. Area of interest for inter-comparison with MODIS is defined in Fig.28 (as in AMTD) and in Table in the Supplement

51. *Supplement 1, there is an "Error! Reference source not found." At the 4th to last line of the first page.*

The sentence is removed

52. *Supplement section 1 and 2, there seems to be no mention of the singleO – oblique angle viewing in the comparison to SURFRAD and Skynet*

Low number (or absence) of matchups in group singleO (most pixels in this group are ocean/coastal pixels) did not allow to perform validation with SURFRAD and SKYNET

References:

LeBlanc, S. E., Redemann, J., Flynn, C., Pistone, K., Kacenelenbogen, M., Segal-rosenheimer, M., Shinozuka, Y., Dunagan, S., Dahlgren, R. P., Meyer, K., Podolske, J., Howell, S. G., Freitag, S., Smallgriswold, J., Holben, B., Diamond, M., Wood, R., Formenti, P., Piketh, S., Maggs-Kölling, G., Gerber, M. and Namwoonde, A.: Above-cloud aerosol optical depth from airborne observations in the southeast Atlantic, Atmos. Chem. Phys., 20, 1565–1590, doi:10.5194/acp-20-1565-2020, 2020.

Sayer, A. M., Hsu, N. C., Lee, J., Kim, W. V., Burton, S., Fenn, M. A., Ferrare, R. A., Kacenelenbogen, M., LeBlanc, S., Pistone, K., Redemann, J., Segal-Rozenhaimer, M., Shinozuka, Y., and Tsay, S.-C.: Two decades observing smoke above clouds in the south-eastern Atlantic Ocean: Deep Blue algorithm updates and validation with ORACLES field campaign data, Atmos. Meas. Tech., 12, 3595–3627, https://doi.org/10.5194/amt-12-3595-2019, 2019.

Shinozuka, Y., Clarke, A. D., Nenes, A., Jefferson, A., Wood, R., McNaughton, C. S., Ström, J., Tunved, P., Redemann, J., Thornhill, K. L., Moore, R. H., Lathem, T. L., Lin, J. J., and Yoon, Y. J.: The relationship between cloud condensation nuclei (CCN) concentration and light extinction of dried particles: indications of underlying aerosol processes and implications for satellite-based CCN estimates, Atmos. Chem. Phys., 15, 7585–7604, https://doi.org/10.5194/acp-15-7585-2015, 2015.

Yoon, J., Von Hoyningen-Huene, W., Kokhanovsky, A. A., Vountas, M. and Burrows, J. P.: Trend analysis of aerosol optical thickness and ngström exponent derived from the global AERONET spectral observations, Atmos. Meas. Tech., 5(6), 1271–1299, doi:10.5194/amt-5-1271-2012, 2012.

York, D., Evensen, N. M., Martınez, M. L., & De Basabe Delgado, J. Unified equations for the slope, intercept, and standard errors of the best straight line. *American journal of physics*, *72*(3), 367-375., https://doi.org/10.1119/1.1632486, 2004.

Response to Stefan Kinne

We thank Stefan Kinne for giving a positive feedback on the revised (based on his comments) version of the manuscript which was published in AMTD

Extended validation and evaluation of the OLCI-SLSTR synergy aerosol product (SY_2_AOD) on Sentinel-3 *by L. Sogacheva et al.*

1 Highlights

- *now inclusion of fine-mode AOD analysis*
- *now much better plots on behavior for different AOD regions*

2 Concerns

- *discussions are too brief (also provide use-recommendations to potential users?)*
  Discussion has been extended.
  Our aim was to perform a critical and detailed evaluation of the Sy_2 product which shows where an improvement of the product is required. Based on this analysis and users needs, they can decide if the product satisfies requirements for their study or not.

- *missing comparisons to the standard SLSTR retrieval (to justify the synergy approach)*
  we reply to this comment below (Specific comments, 119)
- *no fine-mode AOD results in the abstract and fine-mode AOD comparisons to MODIS*
  Results are added
- too extensive comparisons to AERONET
  we aimed to show the performance of the product in different spatial/temporal/geometry conditions and find AERONET is a best choice for that (though we know that AERONET stations are not distributed evenly globally)
- consider AERONET mid-vis AOD <0.04 (and/or remove mountain AERONET site data)
  We answer to this comment below

3 General comments

The paper investigates the performance of a combined OLCI and SLSTR retrievals for AOD, Angstrom (via spectral AOD dependence), AAOD (?), AODf and surface reflection.

The paper investigates the performance of a combined OLCI and SLSTR retrievals for AOD, AOD uncertainty, Angström (via spectral AOD dependence), AODf and FMF. AAOD and surface reflectance are not among validated/evaluated products.

I assume that the SY_2_AOD retrieval performance mainly mirrors for SLSTR covered regions, the SLSTR retrieval performance with a degraded performance in regions, which only the OLCI sensor covers.

AOD in OLCI-only covered areas is not retrieved

Here comparisons and use-statements are at least needed for the discussion section at the end. The discussion section should also address why anyone (user) would want to work with SY_2_AOD in comparison to available data from SLSTR (which still have major issues) and especially over available data from MODIS, VIIRS or MISR.

In the current manuscript we aim for evaluating the SY_2 AOD product. Scatter density plots show the presence of outliers (analysis of the outliers, including identification of the location of outliers, is included in LAW validation report); corresponding validation statistics, binned analysis, fraction of matchups in MODIS EE and fraction of matchups which satisfy GCOS requirements show that improvement of the Sy_2 product is needed. Detailed (regional, dust/single retrieval) analysis allows recognition of the conditions in which product quality is better and where an improvement is needed. Based on the validation results, we do not provide recommendations; users can decide if product quality satisfy the requirements for their study (e.g.,for regional analysis) or not.

I could not find a detailed response to my initial review so some of the concerns I voiced in my initial review are still valid. On the other hand, I very much like in the revised version the new plots that analyze the retrieval performance as function of AOD ranges. These new figures provide much more insights that scatter plots and tables and I suggest to move (the more general performance summaries of) tables (e.g. positive bias but linear fit slope below one seem inconsistent … without the AOD range analysis) and scatter plots - as well as uncertainly analyses into an Appendix or supplement, as the paper is very long and exhausting on the comparisons to AERONET (e.g. I did not know that spectral surface solar reflection is an official AERONET product).

Some figures and tables were moved in the supplement. Scatter density plots are left in the main paper, since they show important information, e.g., a distribution of outliers. We also consider that results from the evaluation of provided uncertainties is important for modellers, who exploit AOD uncertainties in models.

In that context, I also would focus on AERONET data with mid-vis AOD > 0.04 (as lower values are likely related to mountain sites, which should not be considered when comparing to regional data (even for regions as small as 3.5x3.5km areas).

As suggested, we tested removal of the matchups with aAOD<0.04 from the analysis, but the main results (global, for the NH and SH) have not changed considerably. Thus, we keep old results (for all matchups) in the manuscript.

Many important regions for aerosol properties have no or only poor AERONET coverage, so comparisons to global data-sets are essential for a complete pictures. Thus, the effort to compare at the end to a commonly used and likely more mature data-set of MODIS (although potentially with biases, as MODIS AOD overestimates over oceans) is well received, but offered comparisons are way too brief and also miss potentially important AODf comparison (AODf over oceans is offered by the standard MODIS 6.1 product and over land AODf data are available by MODIS-DB AODdust [AODf ~AOD-AODdust] by Pu, B., Ginoux, P., et al., Atmos. Chem. Phys., 20, 55–81, 2020).

We suppose that regions chosen for validation cover most common surface/aerosol conditions globally.

As suggested, we extended FMAOD and FMF evaluation with AERONET.

We also added syFMF and mFMF inter-comparison for test case (26.02.2020).

Validation with ground-based measurements provided valuable information about the product. Extended evaluation with satellite products will be performed when Sy_2 validation results will show a better performance of the retrieval algorithm.

The discussion summary is very brief and disappoints on content, more so since in the data-comparisons, the focus was just on differences and performance with no (or at best little) efforts on interpretations. I strongly suggest to expand the discussion section on major results and their background, so that a reader has a more satisfying element from this comparison paper.

The discussion section on major results was expanded. We added interpretations of the results, where reasons for insufficient quality are clear. However, for some results, interpretation is not possible without painstaking testing of the algorithm performance, which is planned to be done based on the validation results. As suggested by another reviewer, subjective conclusions like “good agreement” were accompanied with quantified results.

4 Specific comments

27 *is there a way to get rid of large outliers (e.g. with a better QA control?)*

AOD quality flags are not provided in the SY_2 product

30 *the abstract does not address high AODf bias (for coarse mode dominated references)*

Results are added

119 *the aim "to allow for a more robust retrieval" needs to be demonstrated (e.g. vs SLSTR)*

Validation results for the SLSTR v1.12 are not published as a paper yet but available on the CCI web-page. We provide a link to those results but do not perform an inter-comparison of the SLSTR and SY_2 validation results in the current manuscript for several reasons:

- we aimed at extended validation with high quality ground-based measurements to evaluate the performance of the algorithm in different conditions. We consider that the results presented describe well the status of the product and allow recognition of the "weak" parts in the retrieval algorithm, which helps in the further development of the retrieval algorithm.
- inter-comparison with the SLSTR, if done properly, requires considerable effort (e.g. pixel-to-pixel, retrieved in both products, inter-comparison; repeating SLSTR validation for the same period when Sy_2 product is available, ets.) which was not covered by the tasks in the LAW project
- We agree that an inter-comparison may add additional information. However, the inter-comparison results should be accomplished with a set of figures and discussion, which will extend considerably the current manuscript, which is already long. Detailed inter-comparison with other satellite products may be a subject for another study/manuscript.

Indeed, some validation statistics for the current version of Sy_2 product (retrieval approach follows the main principles and, with some delay, modifications in the SLSTR retrieval algorithm) are slightly worse compared with SLSTR v1.12 product. However, Sy_2 product is a new product, which is still under development. The validation results reported in the manuscript may also help in further development of the SLSTR AOD product, since the main retrieval approach is simitar for both products.

119 *The aim "to offer data over the entire Sentinel-3 swath" should also be addressed in the discussion (vs SLSTR). I assume similar quality in OCLI only regions over oceans, but significantly reduced quality over OCLI only regions over land.*

Over land the retrieval is performed when both SLSTR and OLCI are available

130 *As different products are offered (e.g. all, dual, nadirS, NadirO) are there reasons why particular versions show be used or avoided in particular regions? If the performance all these different SY versions are addressed, there should be some discussion on their use at the end.*

One product – Sy_2 AOD – is offered. In this product, AOD is retrieved with two different processors, dual or single, depending on the L1b data availability in nadir and oblique views. Based on flags provided, a user can choose which results (if not all) to use. To help users, we provide validation results for different groups of pixels, combined base on the retrieval approach applied.

177 *the Angstrom parameter of the retrieval with AOD at 550 and 865nm over land could be highly inaccurate over vegetation (large/uncertain surf near-IR contributions … any comment?)*

We agree that contribution from the vegetation may be a source for AE errors

295 *aAOD as low as 0.02 permitted? (I would use aAOD>0.04 – as a simple way to exlude mountain sites … although a mountain site exclusion to begin with would be better). I suggest to used aAOD >0.04 only.*

We answered to this comment in the section "General comments"

298 *these biases at low AOD are shocking! Why would anyone want to use that product?*

Our aim was to evaluate the first version of the product and show conditions in which a further development of the retrieval algorithm is needed. Users can decide if the quality of the product is enough for their studies (e.g., if they are interested in regional analysis) or not.

305/315 420/424 528/544 654/660 *scatter plots and tables (and the explanation) in the Appendix as Figures 3/7/13/19 better tell the entire story.*

We agree that Figures 3/7/13/19 better tell the story, but not the entire story. Scatter density plots shows clearly, e.g., the distribution of outliers. This information is hidden in the binned plots (e.g., in Fig.3) .

We moved Tables 2-5 into the supplement.

We also added a new figure, where binned offsets (shown also in Fig.2 as magenta dots) for different groups of products (all, dual, singleN, singleO) are combined into one plot (see below). This kind of visualisation shows clearer offsets to AERONET for pixels retrieved with different approaches and the difference in the results for the NH and SH.

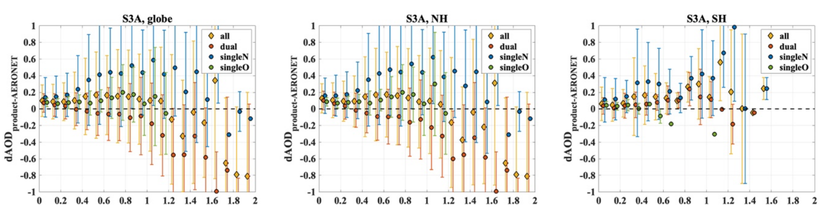

385 *SH Jul-Oct correlation is much better, since (biomass related dry-season) AOD values are higher … so no surprise here.*

Correlation is also good for AOb and Aus, where only low AOD matchups are available

503 *how are uncertainties considered (via weights …?). It is not possible just to remove all data below a specific uncertainty threshold for a higher quality product?*

Uncertainties are considered via weights. AOD quality estimate is not provided in the product. In general, uncertainties can be considered as a quality measure, but provided uncertainties for low AOD are often overestimated.

520 *what is the value of comparing AOD at longer (865 and 1600nm) wavelengths, when aerosol signals are much weaker (or are completely missed when fine-mode aerosol dominates)?*

Often, AE is calculated using AOD_{865}. The knowledge on the AOD_{865} quality is important for explanation of the AE quality.

800 *apparent land-sea contrast in SY data (also easily seen in differences to MODIS) need some explanations. I also strongly encourage to extend such comparisons to the AODf for more insights.*

We included an inter-comparison between syFMF and modFMF (provided in the MOD04_L2 product) for test case described in Sect.8.2 as Fig. 27 in the revised version of the manuscript. Unfortunately, MODIS FMF coverage over land is poor, and thus it can be used for clarification of the difference between syAOD and modAOD.

870 *remove "SKYNET, SURFRAD"*

We decided to mention SKYNET and SURFRAD here. It is mentioned in the paper (in Introduction) that validation was performed also with SKYNET and SURFRAD and that validation results are provided in the supplement.

878 *the discussion (e.g. "Against MODIS, agreement is good") is way too superficial. MODIS overestimates AOD over oceans (compared to MISR, AATSR and AVHRR-DB … and modeling) so that the relative high SY AOD values over oceans, although they compare to MODIS there) are not really encouraging. A closer inspection will also show that SY AOD – also over oceans – are much more fine-mode dominated than most another satellite retrievals (and modeling), which in part causes the land/ocean contrast of Africa for larger dust outflow AOD.*

Validation with MAN shows no bias in SY_ AOD. We add numbers showing the difference between product instead of saying that "agreement is good"

Extended validation and evaluation of the OLCI-SLSTR Synergy aerosol product (SY_2_AOD) on Sentinel-3

Larisa Sogacheva[1], Matthieu Denisselle[2], Pekka Kolmonen[1], Timo H. Virtanen[1], Peter North[3], Claire Henocq[2], Silvia Scifoni[4] and Steffen Dransfeld[5]

[1] Finish Meteorological Institute, Climate Programme, Helsinki, 00540, Finland
[2] ACRI-ST, Sophia-Antipolis, 06410, France
[3] Global Environmental Modelling and Earth Observation (GEMEO), Dept. of Geography, Swansea University, SA28PP, UK
[4] Serco Italia SpA for European Space Agency (ESA), European Space Research Institute (ESRIN), 00044 Frascati, Italy.
[5] European Space Agency (ESA), European Space Research Institute (ESRIN), Frascati, Italy

Correspondence to: Larisa Sogacheva (larisa.sogacheva@fmi.fi)

Abstract

We present the first extended validation of a new synergy global aerosol product (SY_2_AOD) which is based on synergistic use of data from the Ocean and Land Color Instrument (OLCI), and the Sea and Land Surface Temperature Radiometer (SLSTR) sensors onboard the Copernicus Sentinel-3A (S3A) and Sentinel-3B (S3B) satellites. Validation covers period from 14 January 2020 to 30 September 2021. Several approaches, including statistical analysis, time series analysis, comparison with similar aerosol products from the other spaceborne sensor Moderate Resolution Imaging Spectroradiometer (MODIS), were applied for validation end evaluation of S3A and S3B SY_2 aerosol products, including Aerosol Optical Depth (AOD) provided at different wavelengths, AOD pixel level uncertainties, Fine Mode AOD and Angström exponent.

Over ocean, the performance of SY_2 AOD (syAOD) retrieved at 550 nm is good: for S3A and S3B respectively, Pearson correlation coefficients with the Maritime Aerosol Network (MAN) component of the AErosol RObotic NETwork (AERONET) are 0.88 and 0.85; 88.6% and 89.5% of pixels fit into MODIS Error Envelope (EE) of ±0.05±0.2xAOD.

Over land, correlation coefficients with AERONET AOD (aAOD) are 0.60 and 0.63 for S3A and S3B respectively; 51.4% and 57.9% of pixels fit into MODIS EE. Reduced performance over land is expected since the surface reflectance and angular distribution of scattering is higher and more difficult to predict over land than over ocean. The results are affected by a large number of outliers.

Evaluation of the per-retrieval uncertainty with $\chi2$ test indicates, that syAOD prognostic uncertainties (PU) are slightly underestimated ($\chi2 = 3.1$); if outliers are removed, PU describes well the syAOD error ($\chi2 = 1.6$).

The regional analysis of the Angström exponent , which relates to the aerosol size distribution, shows spatial correlation with expected sources. For 40% of the matchups with AERONET in the Northern Hemisphere (NH), and for 60% of the matchups in the Southern Hemisphere (SH), which fit into the AE size range of [1 1.8], an offset between SY_2 AE (syAE) and

Deleted: used
Deleted: fine
Deleted: mode
Deleted:
Deleted: retrieved
Deleted: error
Deleted: envelope
Deleted: *
Deleted: error envelope
Deleted: d good correlation with measured error distributions
Deleted: retrieval
Deleted: o
Deleted: related
Deleted: good

AERONET AE (aAE) is within ±0.25. General overestimation of low (<0.5) syAE and underestimation of high (>1.8) syAE is resulting in high (0.94, globally) overall bias.

Good agreement (bias <0.03) was observed between Sy_2 Fine Mode AOD (syFMAOD) and AERONET Fine mode AOD (aFMAOD) for aFMAOD<1. At aFMAOD>1, syFMAOD is considerably underestimated (by 0.3-0.5 in different aFMAOD ranges) in the NH. In the SH, only few aFMAOD values above 1 are measured. Fine Mode Fraction (FMF) in the SY_2 AOD product (syFMF) in the range of [0 0.7] is overestimated; positive offset of 0.3-0.5 for low (<0.25) FMF is gradually decreasing.

Differences between the annual/ seasonal AOD values from SY_2 and MODIS (mod) Dark Target and Deep blue products are within 0.02 for the study area [30ºS-60ºN, 80ºW-45ºE]. The agreement is better over ocean; however, difference up to 0.6 exists between syFMF and modFMF. Over bright land surface (Saharan desert) the difference in AOD between two products is highest (up to 0.11); the sign of the difference varies over time and space.

For both S3A and S3B AOD products, validation statistics are often slightly better in the Southern Hemisphere. In general, the performance of S3B is slightly better.

5 Introduction

The concern about climate change (e.g., Bergquist and Warshaw, 2019) along with a willingness to reduce its effects (e.g., Leiserowitz et al., 2020; Hoffmann et al., 2022) are of growing interest during the past decades. Global models introduce different scenarios for climate change (Arbor et al., 2021; Meehl et al., 2007), which are often based on the historical records and trends. Satellite data, including aerosols, provide unique global data on the Earth's surface and atmosphere; they are assimilated into global and regional models (Khaki et al., 2020; Eyre et al., 2022) and used for model evaluation (Glìß et al., 2021).

Product quality depends on instrument specifications and applicability of the retrieval approaches. Despite having an advantage in coverage over ground-based products, satellite products often concede lower, compared with ground-based measurements, quality. However, with the fast development of the space-born instruments, including improved quality of onboard instruments and increased temporal and spatial coverage (CEOS, 2017; Dubovik et al., 2021), and on the other hand with improved access to satellite products (Borowitz, 2018) following open access policy (Harris and Bauman, 2015; Olbrich, 2018) and standardisation of satellite data (Loew et al., 2017), the contribution of the space-borne measurements in climate studies is gradually increasing.

Calibration and validation (cal/val) are essential to characterise the quality of the performance of a mission (https://earth.esa.int/eogateway/documents/20142/1564943/Sentinel-3-Calibration-and-Validation-Plan.pdf, last access 14 February 2022). Calibration tasks include pre-launch and in-flight calibrations and characterisation, as well as comprehensive verification of Level-1 data processors. For optical missions, radiometric, spectral, and geometric stability are subjects for investigation.

Deleted: but g

Deleted: ly overestimates

Deleted: AE for cases where AERONET

Deleted: Angstrom is

Deleted: low,

Deleted:

Deleted: high

Deleted: .

Deleted: and

Deleted: .

Deleted: , and

Deleted: h

Deleted: (including aerosols)

Deleted: With

Deleted: Despite having an advantage in coverage over ground-based products, satellite products often concede lower quality. Product quality is an important part of satellite mission requirements. ¶

Deleted: .02.

Validation is a part of a cal/val activity. In the context of remote sensing, validation refers to the process of quantifying the accuracy of satellite retrieved products by assessing the uncertainty of the derived products by analytical comparison to reference data, which is presumed to represent the true value of an attribute. Validation shows the maturity of the satellite derived product and, thus, provides a conclusion on the mission success. Besides providing information about the product quality, validation may reveal a degradation of the instrument or potential drift (Julien and Sobrino, 2021). Validation results should be used in quality assurance reporting together with product details, calibration characterisation, retrieval algorithm description, and uncertainty characterisation.

Validation is a comparison against in-situ measurements, systematic and campaigns, and inter-comparison against other satellite data sources and/or models. Validation requires reference data with high reliability. Since the performance of a retrieval algorithm may vary in different conditions, validation also requires well-sampled coverage of useful ranges of measured values. Possible uncertainties of the product used as the "truth" must be considered. Since other satellite products and models may have their own biases, the inter-comparison against models and other satellite products is called evaluation. Changes in sensors and algorithms may be revealed if similar validation approaches are employed for different versions of products. Thus, common validation principles and approaches should be followed to allow the inter-comparison. General validation is product-specific, while detailed validation is instrument-specific. Validation requires an expertise on instrument, processing, and application, and a good understanding of limitations; thus general validation approaches have to be adapted considering specifications of particular products (e.g., temporal, spatial, radiometric resolutions).

An independent verification processing system is important. The purpose of validation is not only to show how good or bad the product is; issues explaining differences between product and reference data should be identified. Based on validation and evaluation results, recommendations on the product improvements can be provided to the product developers. Recommendations are important as they will help to identify conditions where an algorithm performance should be improved. Iterations on the product validation results with product developers, such as the round robin approach (Holzer-Popp et al, 2013), is a good example on how communication between validation team and product developers should be organised to better utilise validation results for an improvement of product quality.

In this paper we introduce global validation and evaluation results for the Synergy Aerosol Optical Depth (AOD) product, SY_2_AOD (North and Heckel, 2019), for the period from 14 January 2020 to 30 September 2021. The SY_2_AOD product is retrieved from spatially and temporally collocated data measured with two instruments, Sea and Land Surface Temperature Radiometer (SLSTR) and Ocean and Land Color Instrument (OLCI) onboard Sentinel-3 (S3A and S3B) satellites. The synergy retrieval algorithm has been originally developed for the retrieval of AOD from the Advanced Along-Track scanning Radiometer (AATSR) and MEdium-spectral Resolution Imaging Spectrometer (MERIS) (North et al., 2008) and further developed for the S3 instruments. The SY_2_AOD product is available from both S3A and S3B satellites. Extensive and systematic AOD validation against ground-based measurements and inter-comparison with Moderate Resolution Imaging Spectroradiometer (MODIS) AOD product were performed in the frame of the European Space Agency (ESA)

Moved (insertion) [10]

Deleted: However, s

Moved (insertion) [6]

Deleted: the same

Deleted: is applied

Moved down [5]: General validation is product-specific, while detailed validation is instrument-specific.

Moved up [6]: Changes in sensors and algorithms may be revealed if the same validation approach is applied.

Moved (insertion) [5]

Deleted: C

Deleted: objectives

Deleted: ,

Deleted: and challenges

Deleted: applied

Deleted: of validation results and thus, inter-comparison of similar products

Moved (insertion) [7]

Deleted: . However,

Deleted: .

Moved up [10]: Validation requires reference data with high reliability. Possible uncertainties of the product used

Deleted: ¶

Deleted: Possible uncertainties of the product used as the "truth" must be considered.

Deleted: Since the performance of a retrieval algorithm may vary in different conditions, validation also requires well-sampled coverage of useful ranges of measured values.

Moved up [7]: Validation requires an expertise on instrument, processing, and application, and a good understanding of limitations.

Moved down [8]: Iterations on the product validation results with product developers, such as the round robin approach (Holzer-Popp et al, 2013), should be considered to better understand the results.

Moved (insertion) [8]

Deleted: should be considered to better understand the results

Deleted: 01.

Deleted: -09.

Deleted: from 15.01.2020

"ESA/Copernicus Space Component Validation for Land Surface Temperature, Aerosol Optical Depth and Water Vapour Sentinel-3 Products" (LAW, https://law.acri-st.fr/home, last access 10 January 2022).

The paper is structured as following. The SY_2 retrieval algorithm and SY_2_AOD product are introduced in Sect.2. In Sect. 3 we introduce a validation approach applied in the current study. An algorithm developed for extracting satellite and ground-based measurements matchups is explained in Sect.4. Reference validation products are introduced in Sect.4. AOD, AOD uncertainties, Fine mode AOD (FMAOD), Fine Mode Fraction (FMF), Angström exponent (AE) validation results with AERONET are shown in Sect. 6. AOD_{550} validation results with SURFRAD and SKYNET are shown in the Supplement (Sections S1and S2, respectively). Validation results over ocean are presented in Sect. 7. Inter-comparison of daily, monthly, seasonal, and annual SY-2 AOD and MODIS AOD products is shown in Sect. 8. Validation results are summarised in Sect. 9.

6 SY_2 AOD product

6.1 Instrument description

OLCI and SLSTR L1b top-of-the-atmosphere (TOA) radiances were utilized in the SYNERGY algorithm for the retrieval of aerosol properties.

The Sentinel-3 OLCI (https://sentinels.copernicus.eu/web/sentinel/technical-guides/sentinel-3-olci/olci-instrument, last access 16 March 2022) is a push-broom imaging spectrometer with a swath width of 1270 km. It provides spatial sampling at 300 m with five cameras in 21 bands in the spectrum range of 0.4-1.2 µm.

The SLSTR instrument (https://sentinels.copernicus.eu/web/sentinel/technical-guides/sentinel-3-slstr/instrument, last access 16 March 2022) is a conical scanning imaging radiometer employing the along track scanning dual view technique. With the dual view scan (at near nadir and 55° oblique), measurements are taken at nine bands in the range of 0.55-12 µm covering the visible, shortwave infrared, and thermal infrared areas of the spectrum. The SLSTR spatial resolution is 500 m at nadir for visible and shortwave infrared bands and 1km at thermal infrared.

6.2 Algorithm description

The aim of the SYNERGY aerosol algorithm is to provide global aerosol optical depth and related aerosol properties for all cloud and ice-free regions of the Sentinel-3 combined OLCI / SLSTR instrument swaths. The SLSTR retrieval (ESA Aerosol CCI+ portal, https://climate.esa.int/en/projects/aerosol/key-documents/, Algorithm Theoretical Basis Document, last access: 25 February 2022) is of variable quality, with higher uncertainty in retrievals in the oblique backscattering direction. The motivation of combining the SLSTR with OLCI is to improve the SLSTR retrieval using additional spectral information from OLCI. The algorithm is derived originally from the aerosol retrieval algorithm developed by Swansea University under the ESA Aerosol CCI programme for the (A)ATSR and SLSTR instruments (North 2002; Bevan et al., 2012; Popp et al., 2016) but with further development to exploit the increased spectral sampling available from the OLCI instrument. This aims to

Deleted: .01.

Moved (insertion) [9]

Deleted: -8

Moved up [9]: AOD_{550} validation results with SURFRAD and SKYNET are shown in the Supplement (Sections S1and S2, respectively). Inter-comparison of daily

Deleted: 9

Deleted: 10

Deleted: 11

Deleted: SENTINEL

Deleted: .03.

Deleted: .03.

Deleted: ;

Deleted: Product

Deleted: Validation and Intercomparison Report,

Formatted: Underline, Font colour: Blue

Deleted: .02

Deleted: .

Deleted: retreievals

Deleted: on

Deleted: especially in these regions allow a more robust retrieval, but also to provide aerosol estimates over the full Sentinel-3 swath, whereas for the original algorithms using only SLSTR imagery, retrieval over land is only attempted for the regions where both nadir and oblique views are available. The key features of the algorithm are given here and are summarised in detail the SYN AOD Algorithm Theoretical Basis Document (North and Heckel, 2019).

6.2.1 Pre-processing

The algorithm uses the L1c co-registered OLCI and SLSTR data product as input, projected on the OLCI grid. Co-registration is made based on the common 865 nm radiometric band. Over selected ground-control points, radiometric images of SLSTR 865 nm band are extracted and compared to the OLCI 865 nm acquisitions. The OLCI image is moved around according to shift vectors and the cross-correlation with the fixed SLSTR window is calculated. The elements of the shift vectors at which a maximum in cross-correlation is reached determine the pixel deregistration between OLCI and SLSTR reference channel.

Over ocean, AOD is returned using the full swath of the Level 1c (L1c) product (1400 km), while over land the region covered by both nadir and oblique view (750km) is used for best quality retrieval, and aerosol retrieval is also made outside of this region where both nadir-only SLSTR and OLCI is available (~1200 km). Beginning with the L1c product, pixels are flagged to screen cloud, snow ice or sun glint areas. In addition, all neighbouring pixels to cloud pixels are flagged to avoid edge effects. Pixels are grouped into 'super-pixels' formed by blocks of 15x15 pixels of the L1c SYN pixels at 300 m spatial resolution. Thus, a super-pixel represents a resolution of about 4.5 km x 4.5 km. The result is a super-pixel giving aggregated cloud-free TOA radiance for nadir and oblique view (if present) of the same surface location. The inversion is carried out for all land and ocean super-pixels which are at least 50% free of cloud, ice and snow. Over ocean retrieval proceeds if either nadir or oblique super-pixels are valid, while over land both nadir and oblique must be valid for dual view retrieval, or nadir only for single view (spectral) retrieval.

6.2.2 Inversion to derive aerosol parameters

The basis of the algorithm is iterative non-linear optimisation to jointly retrieve aerosol optical depth at a reference wavelength of 550nm, referred to as AOD_{550}, and Fine Mode Fraction (FMF) of AOD_{550}. Atmospheric radiative transfer is approximated as a Look-up Table (LUT) to relate top of atmosphere to surface reflectance, for a given estimate of aerosol parameters, water vapor, ozone and surface pressure. Over both land and ocean, the retrieval requires optimisation of a cost function expressing fit of derived surface reflectance to ocean or land models of reflectance. Several additional parameters are provided, derived from these properties, to provide information on spectral variation of AOD, and surface reflectance values intended as diagnostics (see Sect.2.3 for details). Where a single viewing direction is used, the inversion is made over spectral bands in that direction only. This is normally the case outside the oblique view swath, where nadir only is used, but use of the oblique view alone also occurs over ocean where the nadir view is obscured by glint or cloud. Over ocean, only SLSTR channels (five

Moved (insertion) [4]

Deleted: (i.e., formed from at least 50% of valid pixels)

Deleted: fine

Deleted: mode

Deleted: fraction

Deleted: (FM AOD)

Moved up [4]: The inversion is carried out for all land and ocean super-pixels which are at least 50% free of cloud, ice and snow.

Deleted: Table S1, Supplement

spectral bands, corresponding to S1 (554 nm); S2 (659 nm); S3 (865 nm); S5 (1613 nm) and S6 (2255 nm)) are taken into account in the aerosol retrieval. Over land, both sensors (including OLCI 442.5 nm spectral band) are considered.

A climatology of aerosol composition (Kinne et al., 2013; de Leeuw et al., 2015) is used to provide further information on the fine and coarse components (non-spherical vs spherical, single scattering albedo) and a prior estimate of fine mode fraction. We fit parameters for both AOD and FMF, which controls the spectral variation of AOD. Although AOD is parameterised by a single nominal wavelength (550 nm), all wavelengths of SLSTR, and additionally the 442.5 nm OLCI channel over land are used in this fitting. The SSA is constrained by climatology for the coarse and fine mode extremes separately and as a priori information. The retrieval of FMF results in a SSA by interpolation between these extremes; however, this should be seen as a potential diagnostic for retrieval performance rather than a user product. Further constraints prevent unfeasible retrieval (e.g. negative AOD or surface reflectance). An estimate of the 1 standard deviation (std) error in AOD at 550 nm is derived from the second derivative (curvature) of the error surface near the optimal value.

Deleted: ¶

Deleted: aerosol composition

Deleted: of

Over ocean, a surface reflectance model gives a reflectance estimate determined from the wind speed and direction and using the models of Cox and Munk (1954) for glint, Monahan and O'Muircheartaigh (1980) and Koepke (1984) for foam fraction and spectral reflectance, and Morel's case I water reflectance model dependent on pigment concentration (Morel, 1988). The ocean inversion uses bands from SLSTR only, using both views to invert if both are available, or a single view (either nadir or oblique) where one view is either obscured by cloud, is contaminated by glint, or lies in a swath region where only a single view is present. For land, the reflectance constraint is the result of fitting to separate angular and spectral parameterised models (North, 2002; North et al., 2008; Davies and North, 2015; North and Heckel, 2019). Where the oblique SLSTR view is not available, only the spectral constraint is used, allowing AOD estimation over the full L1c swath over both land and ocean.

6.2.3 Post-processing

A final step is used to filter residual cloud contamination or other sources of poor retrieval. This is based on thresholding of local image standard deviation, discussed in Sogacheva et al., 2017. Over ocean, a final screening is also made on the quality of model fit. Any AOD value outside the AOD valid range of [0, 4] is replaced by a 'fill' value 6.53. 'Clean-air' test is performed to recognise cases when an extensive rejection of low AOD values occurs in case of clean atmosphere, which often happens over dark surfaces. In case this test is positive, which is indicated in quality flags, a value of 0.04 is used.

During post-processing, further aerosol outputs are derived from the retrieved AOD_{550} and FM AOD. This includes spectral variation of AOD, which is given using pre-computed look-up table from the retrieved FM AOD and aerosol mixture. The Angström exponent is computed based on a pair of spectral AOD values. Here we choose 865 nm and 550 nm. A full set of quality flags is provided.

Deleted: derivation of

Deleted: ,

Deleted: such as Angstrom exponent, is performed. Full

6.3 SY_2 AOD product description

Derived aerosol outputs include AOD, AOD uncertainty and single scattering albedo (each at 440 nm, 550 nm, 670 nm, 865 nm, 1610 nm), aerosol absorption optical depth, fine mode AOD, dust AOD (each at 550 nm) and Angström exponent (between

Deleted: duct AOD

550 nm and 865 nm). The full list of derived aerosol outputs which are recorded in gridded NetCDF format at 4.5 km resolution, is shown in Table S1. Additionally for each super-pixel, information is provided giving time and location, solar/view geometry, cloud fraction, AOD retrieval quality flags, and retrieved surface reflectance for each waveband. Quality flags indicate which retrieval method was used, for example nadir-only or dual view, land/ocean algorithm and further indicators such as retrieval failure through negative AOD estimation or glint contamination.

7 Validation approach

The validation approach suggested for the European Space Agency (ESA) Climate Change Initiative (CCI) AOD product validation (ESA Aerosol CCI portal, https://climate.esa.int/en/projects/aerosol/key-documents/, Product Validation and Intercomparison Report, last access: 25 February 2022; de Leeuw et al., 2015) and currently used in ESA Aerosol CCI and Copernicus Climate Change Service C3S_312b Lot2 projects was followed. A similar validation approach has been applied and further developed in Sogacheva et al. (2018a, 2018b, 2020) for validation of the AATSR, MODIS and merged AOD products. The approach includes three main steps: i) match-up between satellite-retrieved AOD and ground-based measurements (Sect.8), ii) statistical tools application to the set of matchups to reveal the agreement between two products (Sect.10) and iii) analysis of the statistics. Different aspects of the validation and evaluation of various AOD products (Chu et al., 2002; Ichoku et al., 2002; Remer et al., 2005; Levy et al., 2013; Shi et al., 2013; Sayer et al., 2012a,b, 2013, 2018, 2019) have been considered. Analysis of the AOD pixel-level provided uncertainties was performed based on the recommendations by Sayer et al. (2020) and considering best practices from the ESA Aerosol CCI.

Annual and seasonal validation was performed globally for all data. Furthermore, respective validations were made over selected areas, which represent different surface and aerosol types.

In the NH, the SLSTR oblique scan generally samples backscattered radiance, which has a weaker aerosol contribution than the corresponding forward scattering sampled in the SH (e.g., https://www-cdn.eumetsat.int/files/2021-09/SARP_Report_Option_1_final.pdf, last access: 25 February 2022). This leads to reduced quality in AOD in the NH compared with SH for the SLSTR products, which has been revealed earlier (https://climate.esa.int/media/documents/Aerosol_cci_PVIR_v1.2_final.pdf, last access: 25 February 2022). For this reason, SY_2 AOD products from the NH and SH were validated separately.

$syAOD_{550}$ validation was performed for all available matchups and separately for groups of the matchups assorted based on prevailing aerosol types. Aerosol types were defined with AERONET AOD (aAOD) and AERONET AE (aAE) thresholds. Although these thresholds are subjective, we consider "background" aerosol to be cases where $aAOD_{550}$ < =0.2, "fine-dominated" with $aAOD_{550}$ > 0.2 and aAE > =1, and "coarse-dominated" with $aAOD_{550}$ > 0.2 and aAE < 1 (e.g. Eck et al., 1999). This classification has also been used by e.g. Sayer et al. (2018) and Sogacheva et al. (2018a, b, 2020).

Another specification of the SY_2 AOD product is that the AOD retrieval has been performed with different retrieval approaches, depending on SLSTR and OLCI coverage and L1B data availability in different viewing angles (for details, see

Deleted: .02.

Deleted: 4

Deleted: 6

Deleted: , and additionally over land and ocean, respectively

Deleted: Since the back scatter contribution to the radiance measured at the top of the atmosphere is more critical in the NH

Deleted:

Deleted: and difference

Deleted: quality

Deleted: between the Northern Hemisphere (NH) and Southern Hemisphere (SH)

Deleted: ,

Sect. 6). Dual-view processor has been applied when SLSTR measurements from both views, nadir and oblique, were available. If measurements were available from one view only, the single view processor was applied to either nadir (over either land or ocean) or oblique view (over ocean or inland waters only). This specification of the product was considered in the current validation exercise.

8 Matchups extraction

A matchup is defined as the combination of simultaneous and spatially collocated satellite and ground-based measurements. Following Ichoku et al (2002), a macro pixel of 11x11 SY_2 AOD pixels (a surface of ca 50 km x 50 km) around each station was extracted at each overpass over a ground-based measurement station. All ground-based measurements were acquired in a time window of ±30 minutes around the satellite crossing time were considered. Statistics such as number of measurements, mean, median, minimum, maximum and standard deviation computed over this time frame were included in the matchup files. All ground-based measurements were extracted from well-qualified networks introduced in Sect. 9.1 (AERONET) , Sect. 9.2 (MAN) and in the supplement (SURFRAD, SKYNET); no additional quality control check has been performed for the reference data. On the contrary, all satellite extractions included all quality flags and contextual parameters presents in the Sentinel-3 operational products. Satellite extractions were created automatically for each station, at each overpass, and centred on the station location. They were then associated with relevant ground-based measurements when these data were available and validated.

"Empty" matchups, i.e., when the whole satellite extraction is associated with a fill value for AOD, were not filtered out from the database, except in case of operational issues in the Sentinel-3 instruments. As these fill values were mainly due to cloud contamination or aerosol retrieval failure, they may provide information about the performance of, e.g., cloud screening in the SY_2 algorithm and were therefore relevant to validation objective.

A free access (upon subscription) to this matchups database has been provided on the ESA LAW web portal (https://law.acri-st.fr/home, last access 10 January 2022).

To explore the performance of different processors, four separate datasets were created and validated separately. The first dataset (called 'all' in the following) consists of all available data, regardless of which processor was used. The second dataset ('dual') contains data retrieved with the dual view processor. The third ('singleN') and fourth ('singleO') dataset are created using the single view processors applied to nadir or oblique views, respectively. The total number of matchups from dual, singleN and singleO groups is higher than the total number of 'all' matchups, because in 11x11 pixels area around reference ground-based measurement there could have been pixels retrieved with different processors (e.g., dual and singleN). In that case we have two matchups (one for dual group and one for single group) for the same spatial-temporal window. If the group not mentioned specifically ('dual', 'singleN' or 'singleO', in the text or in the figure), results are shown and discussed for the group 'all'.

9 Reference datasets

9.1 AERONET

The AERONET is a federation of ground-based remote sensing aerosol networks (https://aeronet.gsfc.nasa.gov/, last access: 25 February 2022). For more than 25 years, AERONET has provided a long-term, continuous, and readily accessible public domain database of aerosol optical, microphysical, and radiative properties for aerosol research and characterization, validation of satellite retrievals, and synergism with other databases. An extensive description of the AERONET sites, procedures and data provided is available from the AERONET web site and in (Holben et al., 1988, Giles et al., 2019).

Ground-based sun photometers directly observe the attenuation of solar radiation without interference from land surface reflections. They provide accurate measurements of AOD with uncertainty ~0.01–0.02 (Eck et al., 1999) in the spectral range of 340-1640 nm.

For the AOD validation, AERONET version 3 data (Giles et al., 2019) – automated near-real-time quality control algorithm with improved cloud screening for Sun photometer aerosol optical depth (AOD) measurements – has been utilized. Version 3 AOD data are computed for three data quality levels: Level 1.0 (unscreened), Level 1.5 (cloud-screened and quality controlled), and Level 2.0 (quality-assured). The Level 2.0 AOD quality-assured dataset is now available within a month after post-field calibration, reducing the lag time from up to several months.

Deleted: -
Deleted: was be
Deleted: L1.0,
Deleted: L1.5,
Deleted: L2.0,

Since AERONET is a network of ground-based sun-photometers, and while some of the AERONET stations are in the coastal land areas and on the islands, open ocean is poorly covered with AERONET. Thus, another available network (see Sect 9.2) is used for validation of AOD retrieved over open ocean.

Deleted: 5.2

9.2 MAN

The Maritime Aerosol Network (MAN) component of AERONET provides ship-borne AOD measurements from the Microtops II sun photometers (Smirnov et al., 2009). These data provide an alternative to observations from islands as well as establish validation points for satellite and aerosol transport models. Since 2004, these instruments have been deployed periodically on ships providing an opportunity for monitoring aerosol properties over the world oceans.

Deleted: aerosol optical depth
Deleted: of opportunity
Deleted: and research vessels to monitor
Deleted:

The Microtops II Sun photometer is a handheld device specifically designed to measure columnar optical depth and water vapor content (Morys et al., 2001). The direct Sun measurements are acquired in five spectral channels within the spectral range 340–1020 nm. The bandwidths of the interference filters vary from 2 to 4 nm (UV channels) to 10 nm for visible and near-infrared channels. The MAN instruments are calibrated against the same reference instruments as utilized in AERONET.

The estimated uncertainty of the optical depth in each channel does not exceed ±0.02, which is slightly higher than the uncertainty of the AERONET field (not master) instruments as shown by Smirnov et al. (2006).

Comparison of MAN and AERONET AOD data does not show any particular bias for AERONET and MAN, although a visible cluster of points above the 1:1 line was acquired in a highly variable dust outbreak conditions west of Africa in the North Atlantic (Smirnov et al., 2011).

9.3 MODIS

Moderate Resolution Imaging Spectroradiometer (MODIS) was launched onboard Terra in 1999. It has a wide spectral range from 0.41µm to 14.5µm, broad swath of 2330 km, and relatively fine spatial resolution of 250 m to 1 km (Levy et al., 2013). The local equator crossing times for MODIS onboard Terra is 10:30.

In this study, the Level 2 combined Dark Target and Deep Blue (DT&DB) AOD product (MOD04_L2) from MODIS Terra collection C6.1 was utilized, which is characterized by good quality and better than Dark Target or Deep Blues coverage alone (Wei et al., 2019).

Deleted: level

10 Validation with AERONET

The AERONET network does not cover the globe evenly. The location of AERONET stations and number of S3A collocations per AERONET station utilized in the validation exercise are shown in Figure 1. For S3B, the number of matchups is similar (slightly higher).

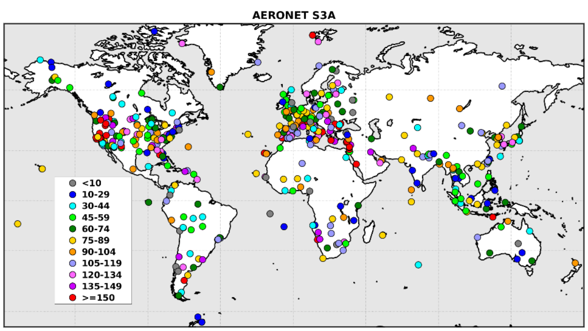

Figure 1: Location of the AERONET stations and number of matchups with S3A, per station (see legend) for the period 14 January 2020 to 30 September 2021.

Deleted: 2020.01-2021.09.

In the exercise it was found that the validation results for S3A and S3B are, in general, similar (difference between results for S3A and S3B is less than 10% of S3A AOD). In this paper, validation results for S3A are shown in figures, while validation statistics for both S3A and S3B (shown as S3A/S3B) are summarised in tables and discussed.

10.1 AOD at 550nm

AERONET does not provide AOD at 550 nm (this dataset will be referred in the following as aAOD$_{550}$). AERONET AOD$_{440}$ (aAOD$_{440}$) and AERONET Angström exponent for 440 nm and 870 nm (aAE$_{440_870}$) are used to calculate aAOD$_{550}$ following the AOD spectral dependence feature (a power law relationship, Angström, 1929). However, aAOD$_{440}$ is not measured at all

AERONET stations. For those stations, aAOD for another wavelength (400 nm or 500 nm) has been used to interpolate aAOD to 550 nm.

As shown in Figure 1, AERONET stations are not evenly distributed globally. For the study period, more than 85% of the matchups were from the NH. Thus, most of global results were strongly influenced by the results obtained for the NH. In case validation results are similar for the globe and the NH, results for the globe are not visualised. In case of a significant difference between the results for the globe and the NH, we show figures and discuss results for both. Validation statistics summarised in tables include results for the globe, NH, and SH.

10.1.1 Annual results

Scatter density plots for S3A SY_2 AOD_{550} ($syAOD_{550}$, or syAOD) and corresponding AERONET AOD_{550} ($aAOD_{550}$, or aAOD) for all matchups available for the NH and SH, including binned AOD offsets, are shown in Figure 2. For most of the matchups (91 %), syAOD is small (<0.4).

Validation statistics (number of points, N; percentage of matchups which fit into MODIS AOD error envelope (EE) defined as ±0.05±0.2xAOD (Remer et al., 2013); percentage of matchups which satisfy Global Climate Observing System (GCOS) requirements of 0.03 or 10% of AOD (GCOS, 2016); Pearson correlation coefficient (R); root mean square (rms); standard deviation, std; bias and slope defined with linear regression (polynomial fit) applied to all available matchups) for S3A and S3B products are shown in Table 1.

A difference in the algorithm performance in the NH and SH is clear. For S3A, the fraction of matchups in the EE (70.8 %) and the fraction of matchups which satisfy GCOS requirements (43.0 %,) are considerably higher in the SH (in the NH, 48.2 % and 20.5 % , respectively), but R (0.62) and rms (0.22) are only slightly better (in the NH, 0.6 and 0.28, respectively). For all matchups, validation statistics are better for S3B: in the SH, more matchups fit to the EE (74.6 %,), GCOS (44.9 %,), R (0.70) is higher, rms (0.15) is lower. In the NH, the difference between S3A and S3B is smaller.

Deleted: , 01.01.2020-30.09.2021,

Deleted: retrieved

Deleted: 0

Moved (insertion) [2]

Deleted: For all matchups, validation statistics are slightly better for S3B (Table 1): more matchups fit to the EE, R is higher, rms, standard deviation and total bias are lower.

Deleted: can be seen

Deleted: T

Deleted: fractions

Deleted: for

Deleted: improved

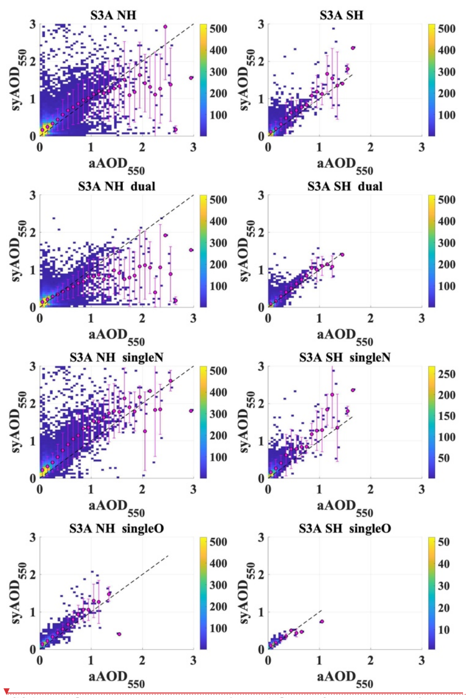

Figure 2: Scatter density plots for S3A syAOD$_{550}$ and corresponding aAOD$_{550}$ for all, dual, singleN and singleO groups of matchups (panels top down) available over the NH (left panel) and SH (right panel). The filled magenta circles are the averaged syAOD binned in 0.1 aAOD intervals and the vertical lines on each circle represent the 1σ standard deviation of the fits.

Deleted: Analysis of the binned (based on aAOD) AOD was performed. For S3A, binned syAOD offset for the smallest aAOD (<0.02) is 0.03-0.05 higher in the NH for all groups (0.11/0.09/0.016/0.08 for all/dual/singleN/singleO) compared with the results for the SH. Offsets in the same AOD range for the S3B are slightly (up to 0.03) lower. For all matchups in the NH small syAOD overestimation (0.07-0.12) is observed for aAOD below 1.2. For 1.2<aAOD<1.5, syAOD is slightly underestimated; for aAOD > 1.5, syAOD is considerably underestimated. However, less than 0.5% of the matchups fit to the range of aAOD>1.5. In the SH, binned syAOD is overestimated.¶

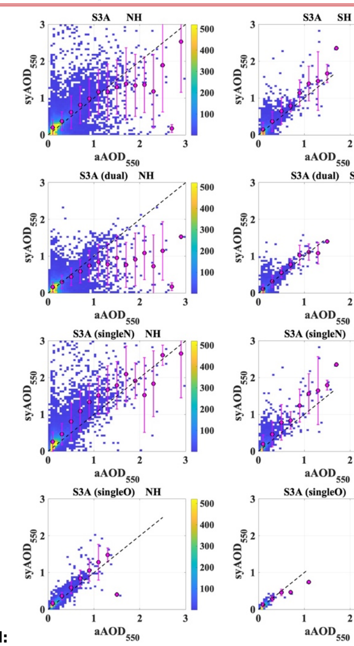

Deleted:

Moved down [1]: For 'dual' group, binned syAOD is lower than aAOD for aAOD> 0.9. For 'singleN' group, positive syAOD offset of 0.2-0.3 AOD is observed when aAOD is in the range of [0.3 1]. For 'singleO' group, offset between syAOD and aAOD is small for aAOD<1.5. Fraction of cases with aAOD>1.5 is very small (only few matchups are available for this group). ¶

Deleted: Validation statistics (number of points, N; percentage of matchups which fit into MODIS AOD error envelope (EE) defined as ±0.05±0.2*AOD (Remer et al., 2013); percentage of matchups which satisfy GCOS requirements of 0.03 or 10% of AOD (GCOS, 2016); correlation coefficient (R); root mean square (rms); standard deviation, std; bias and slope defined with linear regression applied to all available matchups) for S3A and S3B products are shown in Table 1.¶

Table 1 Validation statistics (number of points, N; percentage of matchups which fit into MODIS AOD error envelope, EE, defined as ±0.05±0.2xAOD; percentage of matchups which satisfy GCOS requirements (0.03 or 10% of AOD); correlation coefficient, R; root mean square, rms; standard deviation, σ; bias and slope defined with linear regression applied to all available matchups) for S3A and S3B syAOD$_{550}$ products for the globe, NH and SH for the whole period for all matchups and for three groups of matchups, defined with the processor applied (dual, singleN, singleO).

group	area	N		EE , %		GCOS , %		R		rms		std		bias		slope	
		S3A	S3B	S3A	S3B	S3A	S3B	S3A	S3B	S3A	S3B	S3A	S3B	S3A	S3B	S3A	S3B
all	globe	38376	38829	51.4	57.9	23.8	27.7	0.60	0.63	0.28	0.24	0.001	0.001	0.12	0.10	0.89	0.87
	NH	32856	33240	48.2	55.1	20.5	24.8	0.60	0.62	0.28	0.25	0.001	0.001	0.13	0.11	0.86	0.85
	SH	5520	5589	70.8	74.6	43.0	44.9	0.62	0.70	0.22	0.15	0.003	0.002	0.04	0.04	1.19	1.06
dual	globe	25098	25796	57.9	61.9	29.1	32.1	0.61	0.64	0.19	0.18	0.001	0.001	0.11	0.09	0.62	0.65
	NH	21430	21989	54.2	59.0	25.4	29.3	0.60	0.62	0.20	0.19	0.001	0.001	0.12	0.10	0.58	0.62
	SH	3668	3807	79.3	78.7	50.5	48.3	0.79	0.78	0.12	0.12	0.002	0.002	0.02	0.02	1.07	1.03
singleN	globe	19986	19936	37.9	46.2	14.1	18.1	0.66	0.67	0.35	0.30	0.002	0.002	0.14	0.12	1.20	1.13
	NH	17114	17084	35.5	43.6	11.8	15.4	0.67	0.67	0.36	0.31	0.002	0.002	0.15	0.13	1.19	1.12
	SH	2872	2852	51.7	61.8	27.8	33.9	0.58	0.62	0.30	0.19	0.005	0.003	0.09	0.07	1.31	1.11
singleO	globe	5235	5396	57.7	54.9	20.4	18.3	0.90	0.90	0.11	0.11	0.001	0.001	0.06	0.07	1.12	1.07
	NH	4898	5027	56.2	52.8	18.5	16.0	0.90	0.90	0.11	0.11	0.001	0.001	0.06	0.07	1.12	1.07
	SH	337	369	80.4	82.7	48.7	50.4	0.85	0.88	0.06	0.06	0.003	0.002	0.05	0.03	0.83	1.07

In addition to the statistics shown in Table 1, we performed respective analysis for limited AOD ranges. For aAOD<1.5, syAOD validation statistics are slightly better than statistics for all aAOD ranges: bias is close to 0.1, slope is close to 1 for both S3A and S3B AOD products in the NH. For aAOD>1.5, bias is ca. 1.3 in the NH (where N is 127/125 for S3A/S3B, respectively). In the SH matchups available for S3B product are located close to the 1:1 line, however the number of matchups with aAOD>1.5 is small (N is 3/2) to calculate validation statistics.

Group (dual, singleN, singleO) analysis reveals that most of the low biased syAOD outliers were retrieved with the dual processor (Figure 2), while most of the high biased syAOD outliers were retrieved with the singleN processor. Total bias is smaller for the dual group globally, and in both NH and SH (Table 1). For aAOD<1.5, syAOD bias is close to 0 for the dual group; for the singleN group bias is higher than for all matchups and increasing with aAOD. Validation statistics are, in general, better in the SH (except for R for all the single groups). As for all matchups, validation statistics are slightly better for S3B.

Analysis of the binned (based on aAOD, bin size of 0.1) syAOD offsets to aAOD was carried out. For S3A (Figure 3), the dual group shows better performance. In this group, positive at low (<0.2) AOD offset is vanishing towards higher AOD and turns to negative at AOD>0.4. About 91 % of matchups fit to the AOD range of [0, 0.4]. In this AOD range, an offset is 0.03-0.05 higher in the NH compared with the SH. Offsets for the S3B in the same AOD range are lower (up to 0.03). Offsets for singleN and singleO groups are positive in the AOD range of [0, 1.2]. For high AOD, offsets are in general higher; however, less than 1.4% of the matchups fit to the range of aAOD>1.

Deleted: *

Moved up [2]: For all matchups, validation statistics are slightly better for S3B (Table 1): more matchups fit to the EE, R is higher, rms, standard deviation and total bias are lower.
A difference in the algorithm performance in the NH and SH can be seen. The EE and GCOS fractions are considerably higher for the SH, but R and rms are only slightly improved.

Deleted: applied to the nadir view (group singleN)

Deleted:

Moved (insertion) [1]

Deleted: For 'dual' group, binned syAOD is lower than aAOD for aAOD> 0.9. For 'singleN' group, positive syAOD offset of 0.2-0.3 AOD is observed when aAOD is in the range of [0.3 1]. For 'singleO' group, offset between syAOD and aAOD is small for aAOD<1.5. Fraction of cases with aAOD>1.5 is very small (only few matchups are available for this group).

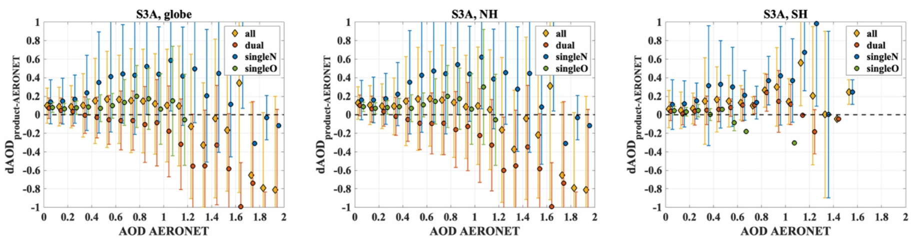

Figure 3: For S3A, binned in 0.1 aAOD intervals, syAOD offsets (dAOD) for the globe, the NH and SH (left to right) for all matchups, dual, singleN and singleO groups of matchups (yellow rhombus, red, green and blue dots, respectively, see legend)

For the aAOD binned on 0.1 intervals, the global difference (dAOD) between syAOD and aAOD represented with the median bias and dAOD standard deviation is shown in Figure 4 for all aerosol types (including background (aAOD ≤ 0.2) AOD), fine-dominated and coarse-dominated AOD. Globally, background AOD (64% from all matchups) is overestimated by 0.04-0.06. Overestimation of fine-dominated matchups is increasing from 0.07 to 0.15 in the AOD range of 0.2-1.2 (34% of matchups). Overestimation for coarse-dominated matchups is about 0.05 for aAOD<0.7; for aAOD of 0.7-0.9, an overestimation for coarse-dominated matchups is within the GCOS requirements of ±0.03 dAOD. For aAOD>1.2, dAOD is varying in the sign and in amplitude; however, the number of matchups in this size range is low (<1 %) and results are thus unstable. Fractions of the fine-dominated matchups per bin is 60-70% for aAOD in the range of 0.2-0.9 and more than 70% for aAOD>0.9. Thus, binned offsets for all matchups follow closely offsets for fine-dominated matchups.

In the NH, the syAOD offset for the background matchups is ~0.07; in the SH the offset is lower (<0.02). Binned offsets for the fine-dominated and coarse-dominated matchups in the NH are similar from those for the globe. In the SH, offsets of syAOD are higher for aAOD>0.4, where the number of the matchups per bin is low (<50).

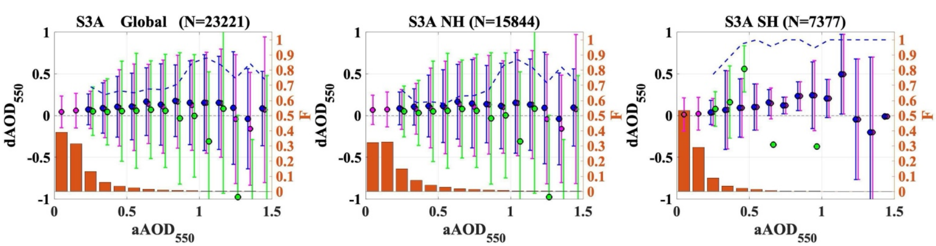

Figure 4: Global, as well as for the NH and SH (left to right), difference (dAOD$_{550}$) between syAOD and aAOD for aAOD binned in 0.2 intervals: median bias (circles) and bias standard deviation (error bars) for all and background (aAOD ≤ 0.2) AOD types (purple), aerosol fine-dominated AOD (blue) and coarse-dominated AOD (green). The fraction (F) of points in each bin from the

Deleted: Global
Deleted: , represented with the median bias and bias standard deviation…
Deleted: Sy_2
Deleted: AERONET monthly AOD
Deleted: for selected aAOD bins are
Deleted: (less than 2% of matchups)
Deleted: the
Deleted: in
Deleted: Fine-dominated matchups dominate over coarse-dominated. …
Deleted: slightly higher (
Deleted:)
Deleted: limited
Deleted: 4
Deleted: difference
Deleted: selected
Deleted: bins

total number of matchups is represented by orange bars. The fraction of fine-dominated matchups in each bin is shown as the blue dashed-line.

10.1.2 Monthly and seasonal results

Monthly (Jan, Feb, Mar, etc.), seasonal (DJF, MAM, JJA, SON) and annual (Year) variation of the validation results for S3A and S3B syAOD$_{550}$ for the globe, NH and SH are shown in Figure 5.

Correlation coefficient R is of sinusoidal shape for monthly statistics with two maxima for both S3A and S3B in the NH. In the SH, correlation coefficient varies strongly along the year. A clear peak (0.8-0.9) for both S3A and S3B is observed in Jun-Oct. Rms in the NH is within 0.25-0.32 for both S3A and S3B, with minimum in Oct-Jan and maximum in Mar-May. In the SH, rms for S3B is 0.15-0.2 in Dec-May and 0.09-0.14 in the other months.

Bias varies from 0.06 to 0.14 in monthly statistics in the NH. In the SH bias is lower; it varies from 0.01 to 0.08 in monthly statistics. For S3B, bias is 0.01-0.35 lower than for S3A in all months, except April.

The fraction of matchups in the EE reflects well the difference between the NH and SH and between S3A and S3B. EE is, in general, higher for S3B with the offset up to 15% in the NH.

As a short summary, syAOD$_{550}$ validation results are slightly better for S3B; retrieval algorithm produces better results in the SH. Obtained validation results confirm that back scatter contribution to the radiance measured at the top of the atmosphere is less critical in the SH.

Deleted: orange

Deleted: For the period 01.2020-09.2021, m

Deleted: are summarised as time series plots in Figure 4.

Deleted: (R_{NH})

Deleted: Peaks in R_{NH} are observed in Feb-Apr (~0.65-0.70) and Aug-Sep. For both S3A and S3B, first clear minimum (0.45-0.47) is observed in Jun; second minimum is observed in Nov-Dec-Jan for S3A (0.48-0.52) and S3B (0.55-0.58).

Deleted: R_{SH}

Deleted: In Dec-May, R_{SH} is between 0.40 and 0.65 for S3B. For S3A, R_{SH}<0.4 in Dec-Mar.¶

Deleted: $_{NH}$

Deleted: $_{SH}$

Deleted: It is higher for S3A, reaching values of 0.25-0.35 in Jan-Feb and Nov-Dec.

Moved (insertion) [3]

Deleted: $_{NH}$

Deleted: .

Deleted: $Bias_{SH}$

Moved up [3]: $Bias_{SH}$ is lower; it varies from 0.01 to 0.08 in monthly statistics.

Deleted: for

Deleted: $Slope_{NH}$ is below 1 in Aug-Jan and above 1 in Apr-May. $Slope_{SH}$ is in general above 1 and is higher than $slope_{NH}$ in Jun. Slope for S3B is lower than for S3A.¶

Deleted: Fraction of the matchups in EE in the SH is considerably higher than in the NH (up to 25% difference) in Feb-Sep, with maximum of 75-82% in the SH in May-Aug for both instruments.

Deleted: show slightly better quality of S3B syAOD$_{550}$

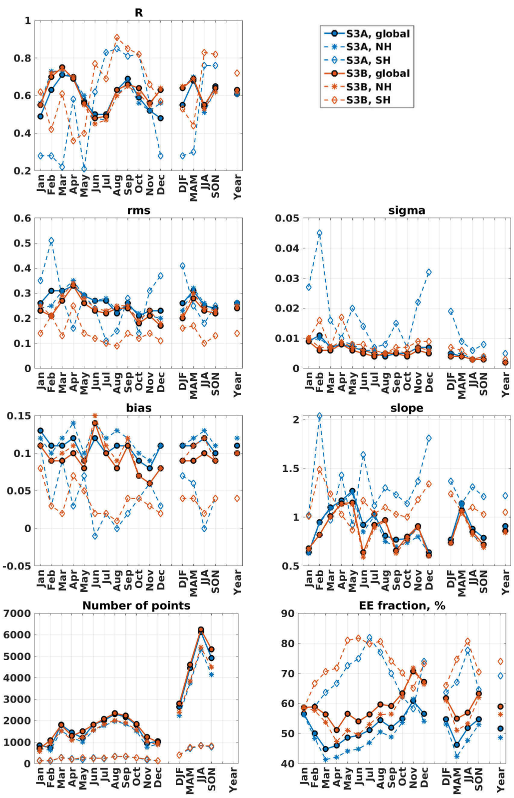

Figure 5: Validation statistics for syAOD$_{550}$ aggregated monthly (Jan, Feb, …, Dec), seasonally (DJF, MAM, JJA, SON) and yearly (Year) shown as time series for S3A and S3B for the globe, NH and SH.

10.1.3 Regional performance

There are noticeable regional differences in the performance of the retrieval algorithm, which depend on, e.g., AOD load and AOD types (composition and optical properties), as well as on the properties of underlying surfaces. Retrieval quality (accuracy, precision and coverage) varies considerably as a function of these conditions, as well as whether a retrieval is performed over land or over ocean.

Following Sogacheva et al. (2020), we inter-compare validation results over 15 regions (as defined in Error! Reference source not found.) that seem likely to represent a sufficient variety of aerosol and surface conditions. These are shown in and

Deleted: **Figure 4: Validation statistics for syAOD$_{550}$ aggregated monthly (Jan, Feb, …, Dec), seasonally (DJF, MAM, JJA, SON) and yearly (Year) shown as time series for S3A and S3B for the globe, NH and SH.**¶

Field Code Changed

Deleted: Figure 6

include 11 land regions, two ocean regions and one heavily mixed region. The land regions represent Europe (denoted by Eur), Boreal (Bor), northern, eastern, and western Asia (AsN, AsE and AsW, respectively), Australia (Aus), northern and southern Africa (AfN and AfS), South America (AmS), and eastern and western Northern America (NAE and NAW). South-Eastern China (ChinaSE), with is part of the AsE, is considered separately. The Atlantic Ocean is represented as two ocean regions, one characterised by Saharan dust outflow over the central Atlantic (AOd) and a second that includes burning outflow over the southern Atlantic (AOb). The mixed region over Indonesia (Ind) includes both land and ocean. For exact locations, see Table S2 in the Supplement.

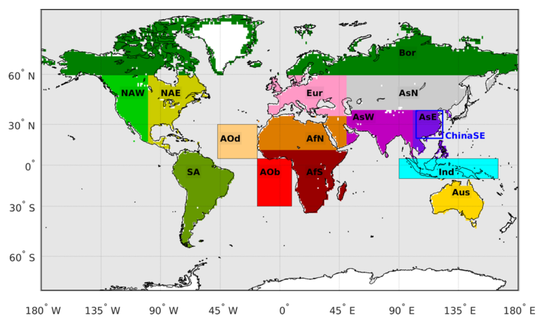

Figure 6: Land and ocean regions defined for this study (as in Sogacheva et al., 2020): Europe (Eur), Boreal (Bor), northern Asia (AsN), eastern Asia (AsE), western Asia (AsW), Australia (Aus), northern Africa (AfN), southern Africa (AfS), South America (SA), eastern North America (NAE), western North America (NAW), Indonesia (Ind), Atlantic Ocean dust outbreak (AOd), Atlantic Ocean biomass burning outbreak (AOb). In addition, Southeast China (ChinaSE), which is part of the AsE region, marked with a blue frame, is considered separately. Land, ocean and global AOD were also considered.

High diversity in the validation results was observed between the selected regions (Figure 7; Table S2 in the Supplement). Highest correlation (0.94) was found in AOb region (the number of matchups is low (22) in this region). For ChinaSE, AsN, AsE, AOd, Aus, NAE, correlation coefficient R was in the range 0.6-0.8, which was higher than that for the globe. For Eur and Ind, R <0.4. For above mentioned regions, bias between binned syAOD and aAOD does not change much. Bias is positive in Asia, Bor and SA regions for aAOD< ~1.2; bias calculated with linear regression was higher for those regions. The amount of syAOD outliers, defined as |syAOD-aAOD| >0.5, varied among the regions. In Eur, positive syAOD outliers were observed for aAOD<0.3. For Asian and Bor regions, syAOD outliers were observed mostly for aAOD in the range of [0.2, 1.2]. More negative syAOD outliers were observed in the NAW region.

Among the land regions, the fraction of the pixels in EE was highest in Aus (81,6%), lowest in Bor and SA (<30%); for other land regions fraction of the pixels in EE was in the 30%-60% interval. Over ocean, in AOb and AOd areas, fraction of the pixels in EE was high (67,8% and 95,5%, respectively).

The fraction of syAOD pixels which satisfy GCOS requirements was low (<31%) for all regions, except for Aus (54,5%) and

Deleted: Figure 7
Deleted: S2
Deleted: Table 2)
Deleted: total
Deleted: that
Deleted: Bias
Deleted: did
Deleted: between the regions
Deleted: between binned syAOD and aAOD was
Deleted: (with only 22 matchups)

AOb (68,2%), where matchups cover low (<0.3) AOD conditions only.

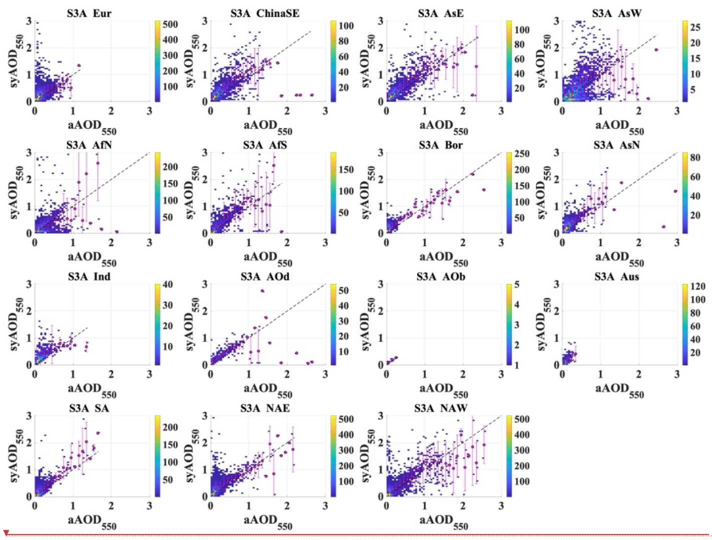

Figure 7: For S3A, syAOD and aAOD scatter density plots for selected regions (as defined in Figure 6).

Regional differences between syAOD and aAOD for all aerosol types (including background (aAOD $\le$ 0.2) AOD), fine-dominated and coarse-dominated AOD for selected aAOD bins are shown in Figure 8. For most of the regions, a general tendency towards positive SY_2 AOD offsets is observed under the background conditions. Offsets are higher (up to 0.15) in Ind and SA and lower (<0.04) in AfN, AfS and AOd. The behavior of the fine-dominated offset is similar for most of the regions (ChinaSE, AfN, AfS, Ind) with gradual increase in the aAOD range of ca 0.7-1.1. Coarse-dominated offset over Eur is underestimated by up to 0.18 for aAOD of 0.6-0.8. Over China, coarse-dominated offset is slightly overestimated at aAOD<0.7 and underestimated at aAOD>1. Over bright surface with contribution of dust aerosols (AfN), all groups show a good agreement with aAOD for aAOD<0.7. For aAOD>0.7, syAOD for coarse-contaminated matchups is considerably underestimated. Similar offsets are observed in NAE region, where 70-90% of matchups are characterized with fine-dominated aerosols. In possible biomass burning region (AfS), an underestimation of syAOD for coarse-dominated matchups gradually increases for aAOD>0.3 reaching -0.9 at aAOD close to 1. Over Ind, dAOD is positive for aAOD <0.5. Over ocean, with possible contamination of Saharan dust (AOd), offsets are constantly positive (up to 0.1) for all groups at aAOD<1.

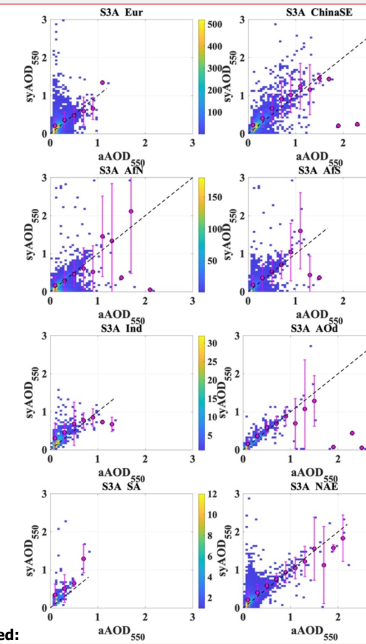

Deleted:

Deleted: Figure 6

Formatted: Check spelling and grammar

Deleted: Region ... [1]

Deleted: A

Deleted: for most regions under the background conditions

Deleted: below

Deleted: slightly

Deleted: positive

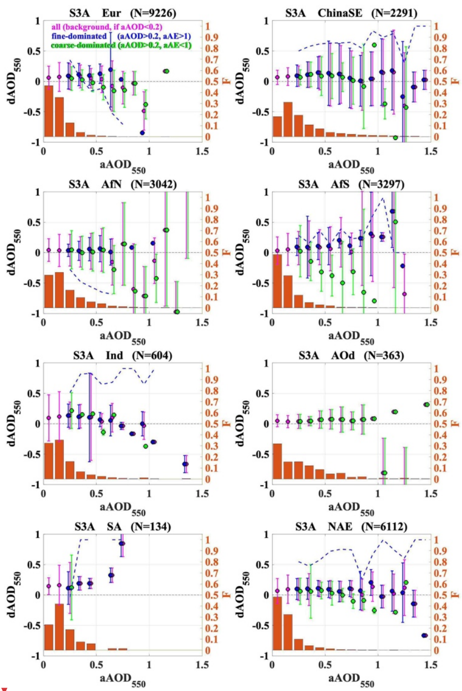

Figure 8: Regional (for Eur, ChinaSE, AfN, AfS, Ind, AOd, SA, NAE) difference ($dAOD_{550}$) between syAOD and aAOD for aAOD binned in 0.1 intervals: median bias (circles) and bias standard deviation (error bars) for all and background (aAOD ≤ 0.2) AOD types (purple), aerosol fine-dominated AOD (blue) and coarse-dominated AOD (green). The fraction (F) of points in each bin from the total number of matchups is represented by orange bars. The fraction of fine-dominated matchups in each bin is shown as blue dashed-line. Results for other regions are in the Supplement (Figure S 7)

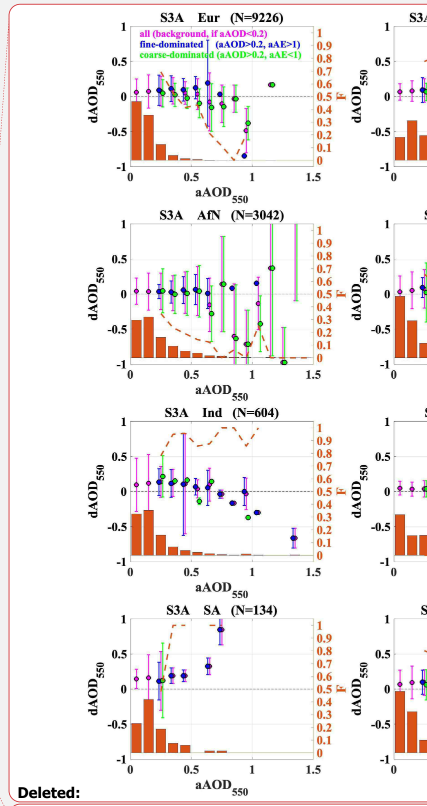

Deleted:

Deleted: selected

Deleted: bins

Deleted: orange

Deleted: 5

10.1.4 Analysis of syAOD relative offsets

syAOD offset analysis was performed for matchups which did not satisfy the GCOS requirements of |syAOD-aAOD|<0.03 or |syAOD-aAOD|<0.1 x aAOD (GCOS, 2016).

syAOD relative offset, or dAOD,rel, was defined as in eq.1:

$$dAOD,rel = \frac{syAOD - aAOD}{aAOD} \quad \text{(eq.1)}$$

10.1.4.1 Latitude dependence of the syAOD relative offset

In Figure 9 we show a density scatter plot for the latitude dependence of the relative offset of the syAOD for all, dual, singleN and singleO groups of pixels for S3A. Colour indicates the fraction of the points with corresponding dAOD,rel from the total number of points within the 10º latitude bin. As an example, for the latitude in [20°S, 30°S], dAOD,rel was between -0.5 and -1 for ~38% of matchups. Magenta line shows the number of matchups in x-axis bin.

In the NH, dAODrel was mostly positive (syAOD was higher than aAOD). In the SH, dAOD,rel is mostly positive in 30°S-60°S and mostly negative in 10°S-30°S, except for the singleN group, where dAOD,rel is mostly positive. In both NH and SH, dAOD,rel is increasing towards the poles. This increase is more pronounced for the singleO group of pixels, but also visible in the dual group.

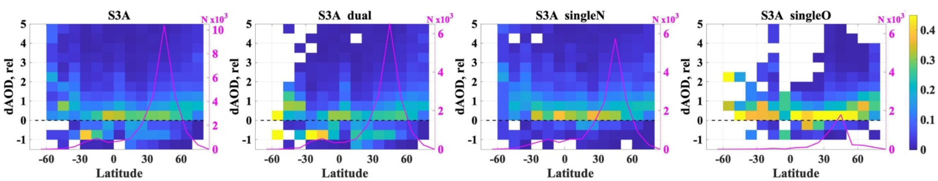

Figure 9: For S3A, density scatter plot for latitude (in degrees) dependence of the syAOD relative offset for 'all', 'dual' and 'singleN' groups of pixels (vertical panels from left to right, respectively). Colour indicates the fraction of the points with corresponding dAOD,rel interval from the total number of points within the latitude bin. Magenta line shows the total number of the matchups in the corresponding latitude bin.

10.1.4.2 Dependence of syAOD relative offset on surface reflectance.

The directional surface reflectance (SR) retrieved with the SYNERGY algorithm is provided in the SY_2_AOD product. In Figure 10 we show a density scatter plot for the dependence of the relative offset of the AOD on the retrieved SR for the dual, singleN and singleO groups of matchups. Colour indicates the fraction of the points with corresponding dAOD,rel from the total number of points within the surface reflectance bin.

For all matchups (not shown here), as well as for the dual group (globally, as well as over the NH and SH), footprints for the dAODrel dependence on the SR are similar. For SR< 0.05 and SR>0.35, dAOD,rel indicates that syAOD is mostly overestimated. In specified ranges, dAOD,rel is increasing towards outer edges. For the SR in the range of 0.05-0.35, syAOD is mostly underestimated. Underestimation is more pronounced when syAOD is retrieved with the dual processor. For the singleO group, syAOD is mostly overestimated in all SR ranges.

Deleted: ¶
dAOD$_{rel}$ = (syAOD-aAOD)/aAOD (eq.1)¶
syAOD offset analysis was performed for matchups which did not satisfy the GCOS requirements of |syAOD-aAOD|<0.03 or |syAOD-aAOD|<0.1*aAOD (GCOS, 2016).¶

Deleted: and S3B products

Deleted: -

Deleted: -20

Deleted: which means 20°S-30°S,

Deleted: ca

Deleted: (colorbar)

Deleted: was

Deleted: was

Deleted: was

Deleted: was

Deleted: Figure 9

Deleted: globe, NH and SH

Deleted: as on Figure 9,

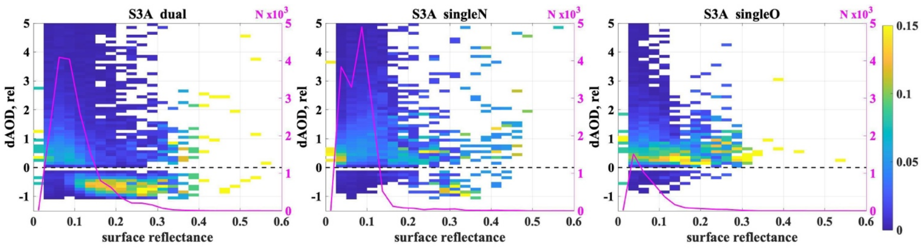

Figure 10: For S3A, syAOD matchups with AERONET which do not satisfy GCOS requirements, scatter density plot for the dependence of the syAOD relative offset of retrieved surface reflectance for 'all', 'dual' and 'singleN' groups of pixels (vertical panels from left to right, respectively). Colour indicates the fraction of the points with corresponding dAOD,rel interval from the total number of points within the surface reflectance bin. Magenta line shows the total number of the matchups in the corresponding surface reflectance bin.

10.1.4.3 Dependence of the AOD relative offset on solar and satellite geometry

In Figure 11Figure 11 we show the dependence of the syAOD relative offsets on the OLCI geometry (relative azimuth (Raz), satellite zenith angle (SatZA) and sun (or solar) zenith angle (SunZA) provided in the SY_2_AOD product, North and Heckel, 2019) for the NH and SH. Colour indicates the fraction of the points with corresponding dAOD,rel interval in the Raz, SatZA, or SunZA bins.

In the NH, positive dAOD,rel is increasing for Raz in [50°, 80°] and in [100°, 140°]. In the SH, we see the similar dependence of dAOD,rel for Raz in [50° 80°]. For Raz>90°, positive dAOD,rel is increasing with Raz increase from 150° to 180°; negative dAOD,rel of [-1, -0.5] is observed more often than positive [0 0.5] dAOD,rel.

No significant dependence of dAOD,rel on the SatZA was observed. However, a greater number of negative dAOD,rel is clearly seen in the SH.

In the NH, dAODrel is slightly positive (0-0.5), in all range of SunZA, except for the most extreme values. For SunZA>80°, the percentage of higher positive dAOD,rel (0.5-1) increases, while for SunZA<30° the percentage of higher negative dAOD,rel rises. In the SH, similar dependence was observed, except for SunZA in the range of 50°-65°, where dAOD,rel is mainly negative.

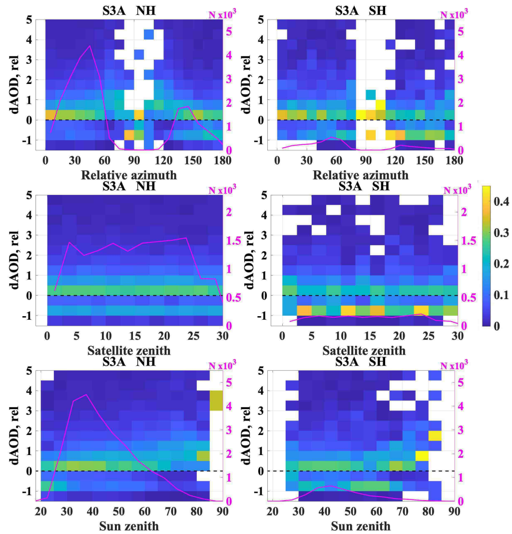

Figure 11: For S3A, syAOD matchups with AERONET which do not satisfy GCOS requirements, the dependence of the AOD relative offsets on relative azimuth (upper panel), satellite zenith angle (middle panel) and sun zenith angle (lower panel) for the NH (left panel) and SH (right panel) for all pixels. Colour indicates the fraction of the points with corresponding dAOD rel from the total number of points within the x-axis bin. Magenta line shows the total number of the matchups in the corresponding x-axis bin.

10.1.5 Linear regression considering provided syAOD uncertainties

Linear fitting for combinations of $syAOD_{550}$ and $aAOD_{550}$ collocations has been performed with a consideration of the $syAOD_{550}$ and $aAOD_{550}$ uncertainties (https://se.mathworks.com/help/stats/linearmodel.predict.html, last access 08 March 2022). For $syAOD_{550}$, pixel-level uncertainties are provided in the SY_2_AOD product. For $aAOD_{550}$, uncertainty of 0.01 has been considered (Eck et al., 1999). For both S3A and S3B, for all groups of matchups, bias and slope for the linear regression fits applied to the whole AOD range were improved when the syAOD and aAOD uncertainties were considered. Bias was lowered roughly by 50%. Slope was improved by 10-15%. Improvements were smaller for singleO group of matchups (retrievals over ocean), for which the syAOD uncertainties are smallest (Sect. 10.2).

For more details, see Fig. S7 and Table S3, both in the Supplement.

10.1.6 AOD at other than 550nm wavelengths

Deleted: .03.

Deleted: ¶
In Figure 11 we show linear fit for $syAOD_{550}$ and $aAOD_{550}$ without (green line) and with (red line) considering the provided $syAOD_{550}$ uncertainties for all matchups and groups of pixels retrieved with different (dual, single) approaches. Corresponding statistics (bias, slope) are provided in Table 3.¶

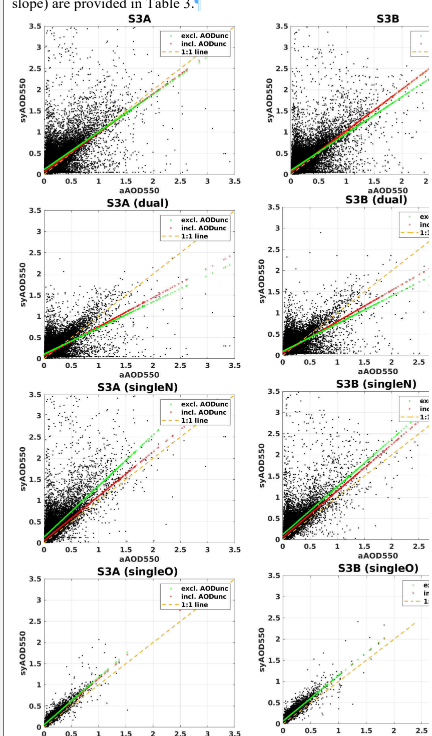

Figure 11: For S3A (left panel) and S3B (right panel), linear fit without (green dotted line) and with (red dotted line) considering $syAOD_{550}$ and $aAOD_{550}$ uncertainties. Dashed orange line is 1:1 line.¶

Deleted: 6.2

Deleted: **Table 3: Validation statistics (bias, slope) for groups of pixels for $syAOD_{550}$ and $aAOD_{550}$ without and with consideration of AOD uncertainties**¶

... [2]

Scatter plots for SY_2 AOD_{440}, AOD_{670}, AOD_{865}, and AOD_{1600} are shown in Figure 12Figure 12. Clear tendencies in validation statistics were observed when comparing validation results from shorter (440 nm) to longer (1600 nm) wavelengths. Though the correlation coefficient is decreasing (0.65/0.55/0.50/0.40 for 440/670/865/1600 nm respectively), the offset (0.15/0.1/0.07/0.05/) and rms (0.33/0.23/0.18/0.16) are also decreasing. Note, that AOD is decreasing significantly (except for dust aerosols) as wavelength increases.

Validation statistics for all wavelengths are slightly worse for the NH than global validation statistics (Table S4, Supplement); validation statistics for the SH are considerably better than for the NH (except for R for 1600nm wavelength).

Deleted: Table 4

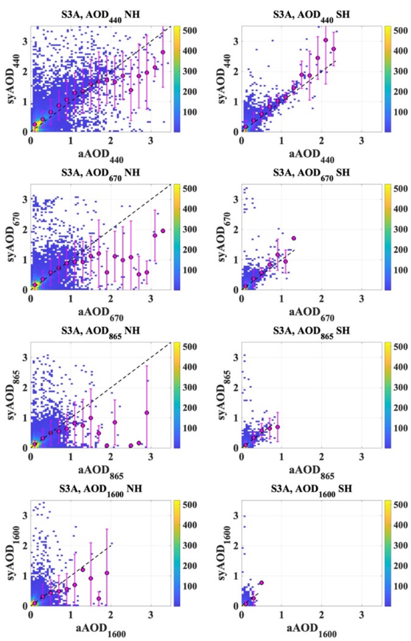

Figure 12: Scatter plots for SY_2 AOD_{440}, AOD_{670}, AOD_{870}, and AOD_{1600} (panels top down) for the NH and SH (left and right panels, respectively).

$syAOD_{440}$ is overestimated for all aerosol types (Figure 13**Figure 13**). $syAOD_{670}$ for fine-dominated matchups is in a good agreement with $aAOD_{670}$ for $aAOD_{670}$<1. Similar tendency, though for narrower aAOD ranges ($aAOD_{870}$<0.5 and $aAOD_{1600}$<0.3), is observed for $syAOD_{865}$ and $syAOD_{1600}$. For all wave lengths, coarse-dominated syAOD is retrieved accurately for aAOD below ca. 0.4; above 0.4 syAOD is underestimated and offset between syAOD and aAOD is increasing with increasing aAOD.

Formatted: Font: 10 pt, Not Bold

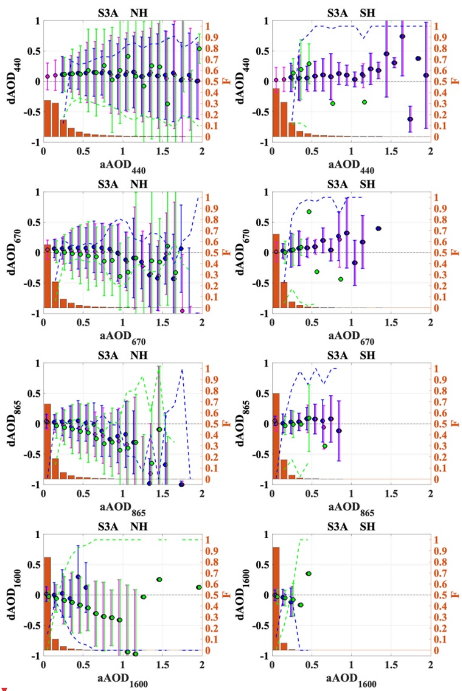

Figure 13: for the NH (left) and SH (right), for different wavelengths (top down: 440, 670, 865, 1600 nm), the difference ($dAOD_{550}$) between syAOD and aAOD for selected aAOD bins: median bias (circles) and bias standard deviation (error bars) for all (incl. background, $aAOD_{550} \leq 0.2$) AOD types (purple), aerosol fine-dominated AOD (blue) and coarse-dominated (green) AOD. The fraction (F) of fine-dominated matchups from the total number of matchups in each bin is represented by orange bars. The fraction of fine- and coarse-dominated matchups in each bin is shown as blue and green dashed-lines, respectively.

10.2 AOD uncertainties

The concept for validation of the AOD uncertainties applied in the current study follows the validation strategy suggested by Sayer et al. (2013, 2020) with consideration of the validation practice further developed in the ESA Aerosol_cci+ project (Product Validation and Intercomparison Report, https://climate.esa.int/media/documents/Aerosol_cci_PVIR_v1.2_final.pdf, last access: 25 February 2022).

Definitions for uncertainties in the current evaluation of uncertainties are as following:

Deleted:

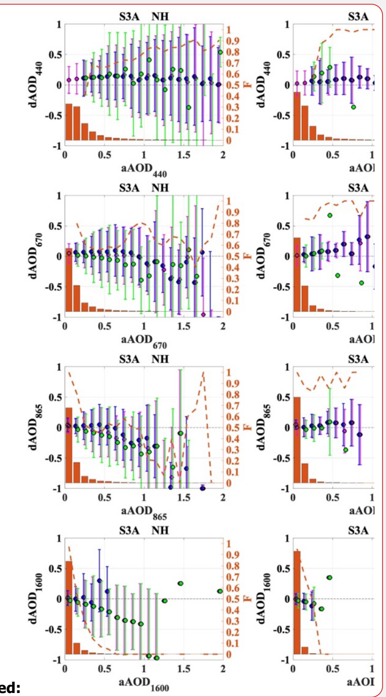

Deleted: left to

Deleted: orange

Deleted: Table 4: For S3A, for different wavelength regional validation statistics: number of points, N; percentage of matchups which fit into MODIS AOD error envelope for AOD_{550}, EE; percentage of matchups which satisfy GCOS requirements; correlation coefficient, R; root mean square, rms; standard deviation, sigma; bias and slope defined with linear regression applied to all available matchups.
wavelength, nm ... [3]

Deleted: 5.02.

- Prognostic (per-retrieval) uncertainties (PU) for SY_2_AOD product are provided at 440, 550, 670, 865, 1600 and 2250 nm wavelengths.
- Expected discrepancy (ED) is an uncertainty variable which accounts for the PU and the accuracy of the ground-based (AERONET) data (AU), as defined by Sayer et al. (2020) in eq.2:

  $$ED = \sqrt{PU^2 + AU^2} \text{ (eq.2)}$$

  According to Giles et al. (2019), AU = 0.01.
- AOD error (AODerror) is a difference between satellite product AOD (syAOD) and AERONET AOD (aAOD); AOD absolute error (absAODerror) is an absolute value for AODerror.

Mean-bias correction has been performed for the error distributions in some of the subsequent analysis, since the concept of standard uncertainties requires bias-free error distributions which can be interpreted as absence of remaining systematic and quantifiable biases (https://climate.esa.int/media/documents/Aerosol_cci_PVIR_v1.2_final.pdf, last access: 25 February 2022).

Deleted: 5.02.

If wavelength is not specifically mentioned, all variables in Section 6.2 are referring to the wavelength of 550 nm.

Analysis of the distribution of the uncertainties has been performed for the whole S3A and S3B SY_2_AOD product, as well as for groups of pixels retrieved with different retrieval approaches (dual, singleN, singleO). Results for S3A and S3B are similar; only results for S3A are shown and discussed.

10.2.1 χ2 test for evaluation of the prognostic uncertainties

The goodness of the predicted uncertainties was estimated with the χ2 test, as in eq.3

$$\chi 2 = \frac{1}{N-1}\sum_{i=1}^{N}\delta_i \quad \text{(eq.3)},$$

where individual weighted deviation δ_i is described in eq.3.

$$\delta_i = \frac{(syAOD_i - aAOD_i - mean(syAOD - aAOD))^2}{PU_i^2 + AU^2} \quad \text{(eq.4)}$$

If χ2 ~1, prognostic uncertainties describe well the AODerror. If χ2 >>1, PU are strongly underestimated; if χ2 <<1, PU are strongly overestimated. χ2 was calculated for the whole dataset and for different AOD bins to reveal if the goodness of the PU uncertainties is AOD dependent.

For the whole dataset, χ2 =3.1, which means that PU are slightly underestimated. For the binned AOD, χ2 is varying strongly (Figure 14). For aAOD<0.4, which is ca 90 % of all values, χ2 fits into the interval [1.8 3.2]. Thus, for most of the matchups, PU is only slightly underestimated. For AOD>0.4 PU underestimation is more pronounced.

No significant dependence of δ_i on AODerror or surface reflectance provided in the SY_2_AOD product has been revealed (Figure S 6, Supplement).

Though the number of the matchups in the whole dataset is high (which provides the confidence to χ2 test results), it was noticed that high δ_i (up to 155) exists, which may bias the evaluation of the PU with χ2. To remove possible contribution of the outliers on the $\chi 2$ test results, cases with $\delta_i > 10$ (which are less than 5 % of the total number of matchups) were removed from the analysis.

For the dataset with the removed outliers, $\chi 2$ =1.2, which means that PU describe well the AODerror.

Influence of δ_i outliers is more pronounced for AOD bins, where the number of matchups per bin is lower and thus the contribution of the outlies to the results is more expected. If δ_i outliers are removed from the binned analysis, $\chi 2$ fits to the range [1 1.45] for AOD<0.4 (Figure 14).

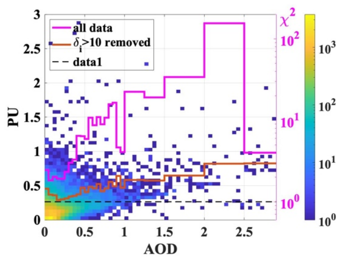

Figure 14: $\chi 2$ for binned aAOD for all available matchups (magenta line) and after the outliers of the individual weighted deviations (δ_i>10) are removed (red line). Density scatter plot for PU and syAOD.

10.2.2 Evaluation of prognostic uncertainties with absolute AOD error

To qualitatively illustrate an accuracy of prognostic uncertainties, we show in Figure 15 the comparison between the PU, AOD error distribution, and theoretical Gaussian distribution (with a mean of 0 and standard deviation of the syAODerror). PU distribution shows a double peak, (first peak is at ca. 0.02-0.04 for all groups; the second peak in a range of 0.12-0.18, for different groups). For singleN, two peaks are located close to each other. Mean PU for dual group is higher; std is higher for singleN group. AOD error distributions are Gauss-like with partly some asymmetry in positive AODerror direction.

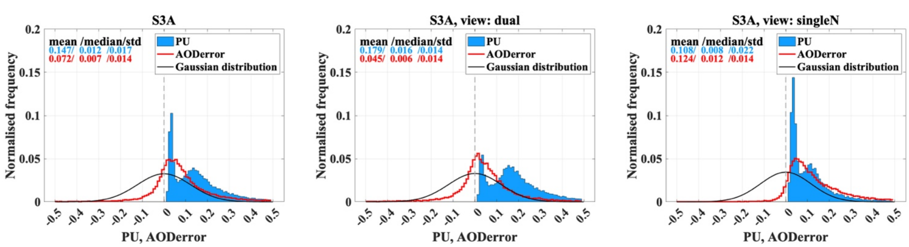

Figure 15: Comparison between PU, AOD error distribution and theoretical Gaussian distribution for the whole product (left panel), dual- (middle panel) and singleN (right panel) groups of matchups.

Deleted: Figure 15

10.2.3 Evaluation of expected discrepancy and absolute AOD error

ED is calculated for each pixel by combining PU and AERONET uncertainties, as in eq.2.

For a quantitative validation, we follow (with some modifications) a new approach developed by ESA Aerosol CCI (https://climate.esa.int/media/documents/Aerosol_cci_PVIR_v1.2_final.pdf, last access: 25 February 2022). A synthetic cumulative distribution of ED is calculated assuming a Gaussian error distribution (normalized to a total integral of 1) with standard deviation of ED. In the next step, this synthetic error frequency distribution is compared with the AODerror. We calculate and subtract the mean bias from the AODerror distribution to make it more symmetric for direct comparison to the synthetic distribution (which by its definition is always symmetric). Bias correction results for S3A all, dual and singleN (0.07, 0.04 and 0.12, respectively) are shown in Figure 16Figure 16.

Finally, we calculate an average correction factor for the synthetic distribution (and thus the prognostic uncertainties) in relation to the mean-bias corrected error distributions as the ratio of the absolute means of both distributions. Corrections factors are different for all matchups, dual and singleN groups. A small correction is needed for all and singleN (0.80 and 1.1, respectively). For the dual group, the correction is stronger (0.67); ED should be lowered.

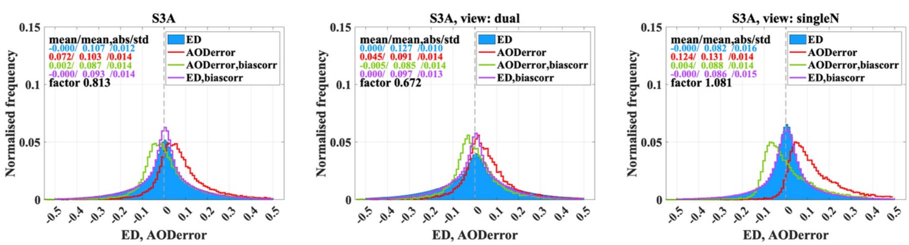

Figure 16: Histograms of the ED (blue filled bars), AODerrors (red; with bias correction: green) and ED calculated from uncertainties (purple; scaled to best fit the mean-bias corrected error distribution) for all matchups (left panel), dual- (middle panel) and singleN (right panel) groups of matchups. Statistics, mean/mean,abs/std are mean over 'real' values, mean over 'absolute' values and standard deviation, respectively, for histograms of the corresponding color.

However, the correction method applied here is not equally improving ED in all ranges. The correction factor is biased by the number of pixels with small (<0.2) absAODerror. Thus, for those cases the correction works well; overestimated ED is lowered by 0.8/0.65 for all and dual groups. For absAODerror > ca.0.3, where ED is underestimated, correction degrades ED and increases disagreement between ED and AODerror. Possible solution can be in performing correction separately for different absAODerror ranges but setting specific relations for different groups between ED and absAODerror makes the analysis very complicated.

Deleted: .02.

Deleted:

10.2.4 Potential of the expected discrepancy

Sayer et al. (2020) suggested the analysis of the potential of the PU to discriminate between (‘good’ and ‘bad’) pixels with likely small / large errors. Instead of PU, we perform analysis of the ED, which, besides PU, includes uncertainties of the ground-based measurements.

To estimate the potential of ED, we plot the absolute errors below which 38% of all pixels are, as a function of binned ED (Figure 17Figure 17). We then repeat this for the fractions 68% and 95%. These percentages relate to 0.5σ, 1σ, and 2σ (where σ is a standard width) for normal error distributions in each bin (along the vertical axis). Theoretically expected values are shown as dashed lines in black, red, and blue. The number of pixels per ED bin is shown as a grey dashed line.

The percentile plots show a reasonable agreement (within statistical noise) with the theoretical lines of 38% and 68% for majority of the validation points in the lower range of ED (up to 0.05-0.2) for all groups, with underestimation of the true error at higher values of ED for 38% and 68% lines. For the dual view case, ED overestimates the true error, while for the single view case the true error is higher than the ED prediction, especially at higher values of ED (ED>~ 0.2).

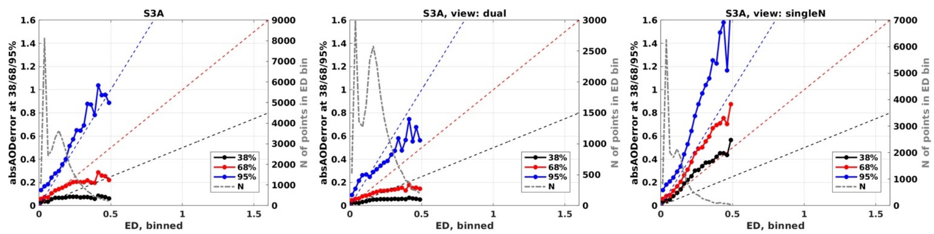

Figure 17: Percentile plots of absAODerrors at 38% (black), 68% (red) and 95% (blue) as function of binned expected discrepancy.

10.3 Fine mode AOD and Fine Mode Fraction

Fine mode AOD in the SY_2 product (syFMAOD) is provided at 550nm, while AERONET Fine mode AOD (aFMAOD) is provided at 500 nm. As for aAOD$_{500}$ (Sect. 10.1), AOD spectral dependence (https://aeronet.gsfc.nasa.gov/new_web/man_data.html, O’Neill et al., 2003, last access: 25 February 2022) and AERONET AE exponent were considered to convert aFMAOD$_{500}$ into aFMAOD$_{550}$.

Density scatter plots for the relation between syFMAOD and aFMAOD in the NH and SH, are shown in Figure 18Figure 18 for S3A; validation statistics are summarised in Table 2 for both S3A and S3B. The dispersion of points is higher in the NH. Validation results are considerably better in the SH: R is higher (0.67 vs 0.63 for the SH and NH, respectively), rms (0.15 vs 0.23) and bias (0.06 vs 0.14) are lower, slope (0.93 vs 0.70) is closer to 1. Analysis of the binned FMAOD shows that in both NH and SH, good agreement was observed between syFMAOD and aFMAOD for aFMAOD<1. At aFMAOD>1, syFMAOD is considerably underestimated in the NH. In the SH, only few aFMAOD values above 1 are measured. Validation statistics for S3B are slightly better.

Deleted: Figure 17

Deleted: ,

Deleted: was

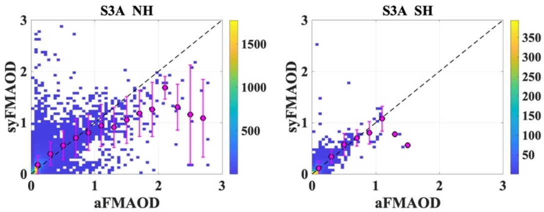

Figure 18: Density scatter plots for S3A syFMAOD and corresponding aFMAOD for collocations available over the NH (left) and SH (right).

Looking at the seasonal validation results, for both S3A and S3B, the correlation coefficient is slightly higher in MAM (0.65 /0.67, for S3A/S3B, respectively) and JJA (0.67/0.69) and lower (0.56/0.59) in DJF (Table 2; Figure S9, Supplement). Bias is ca 0.1-0.12 and slightly higher (0.15/0.12) in JJA. The binned mean syFMAOD values are close to the 1:1 line for aFMAOD < 0.6-1 but fall below the line for higher aFMAOD.

Table 2: For S3A and S3B, annual (for the globe, NH and SH) and seasonal (for the globe) validation statistics for syFMAOD.

Period	Region	N		R		rms		std		bias		slope	
		S3A	S3B	S3A	S3B	S3A	S3B	S3A	S3B	S3A	S3B	S3A	S3B
year	globe	18145	18262	0.63	0.67	0.22	0.20	0.001	0.001	0.13	0.12	0.72	0.72
	NH	15883	15982	0.63	0.66	0.23	0.20	0.002	0.001	0.14	0.12	0.70	0.71
	SH	2262	2280	0.67	0.72	0.15	0.15	0.003	0.002	0.06	0.06	0.93	0.91
DJF	globe	2447	2418	0.56	0.58	0.21	0.18	0.004	0.003	0.12	0.10	0.59	0.53
MAM		5832	5952	0.65	0.67	0.22	0.21	0.002	0.002	0.12	0.11	0.85	0.86
JJA		7641	7579	0.67	0.69	0.23	0.20	0.002	0.002	0.1	0.13	0.71	0.70
SON		2225	2313	0.49	0.66	0.22	0.16	0.004	0.003	0.12	0.10	0.56	0.62

Among selected regions, offset for all aerosol types is negligible (slightly positive) in Eur, Ind and NAW (Figure 19). In ChinaSE and AfN, an offset is increasing with increasing of aFMAOD over 0.5 and becomes more unstable (takes both positive and negative values).

Deleted: Table 2

Deleted: (Figure 19), regional

Formatted: Font: 10 pt

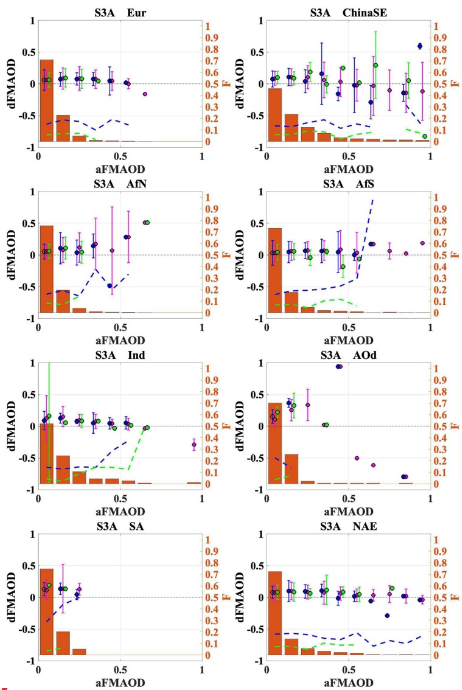

Figure 19: Regional (for Eur, ChinaSE, AfN, AfS, Ind, AOd, SA, NAE) difference (dFMAOD) between syFMAOD and aFMAOD for selected aFMAOD bins: median bias (circles) and bias standard deviation (error bars) for all AOD types (purple), aerosol fine-dominated AOD (blue) and coarse-dominated AOD (green). The fraction (F) of points in each bin from the total number of matchups is represented by orange bars. The fraction of fine-dominated matchups in each bin is shown as orange dashed-line. Results for other regions are in the Supplement (Figure S 10).

Deleted:

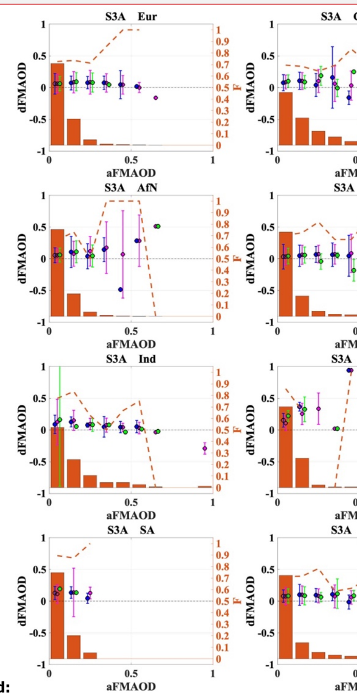

SY_2 Fine Mode Fraction (syFMF), which is a fraction of syFMAOD from the total syAOD, was validated against AERONET Fine Mode Fraction (aFMF). Since syFMAOD is slightly overestimated, we expect that syFMF is overestimated as well. Density scatter plots for the relation between syFMF and aFMF in the NH and SH are shown in Figure 20 for S3A. In both hemispheres, and thus globally, syFMF is overestimated in the aFMF range of 0-0.7; positive offset of 0.3-0.5 at low (<0.25) aFMF is gradually decreasing. At aFMF>0.9, syFMF is slightly underestimated. Offset between syFMF and aFMF is slightly lower in the SH. For the NH/SH respectively, R is 0.34/0.42; bias is 0.56/0.49, slope is 0.28/0.37.

Formatted: Font: 10 pt

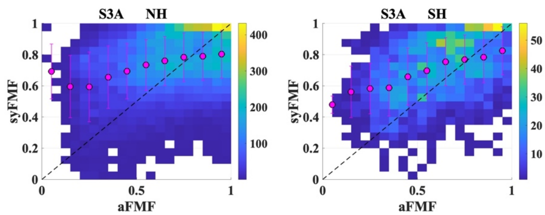

Figure 20: Density scatter plots for S3A syFMF and corresponding aFM for collocations available over the NH (left) and SH (right).

Scatter density plot between dFMF (which is defined as a difference between syFMF and aFMF) and aAOD is shown in Figure 21 for the NH and SH. In general, offset is higher at low AOD and decreases towards high AOD. The fraction of high (>0.05) overestimates is decreasing towards high AOD, while the fraction of high underestimates increases.

Deleted: in

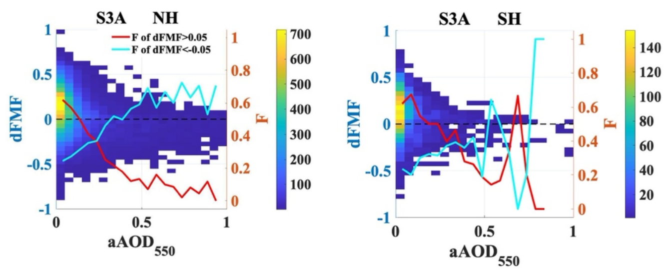

Figure 21: Density scatter plot for the difference (dFMF) between syFMF and aFMF as a function of $aAOD_{550}$. Fractions of positive (dFMF>0.05, red line) and negative (dFMF<-0.05, blue line) overestimations per aAOD bin are shown.

Regional dFMF (Figure 22) is positive (0.3-0.7) for low (<0.2) aFMF and decreasing gradually towards higher aFMF. At aFMF above 0.5-0.7, aFMF turns to negative (syFMF is underestimated). Similar tendency is observed for all chosen regions.

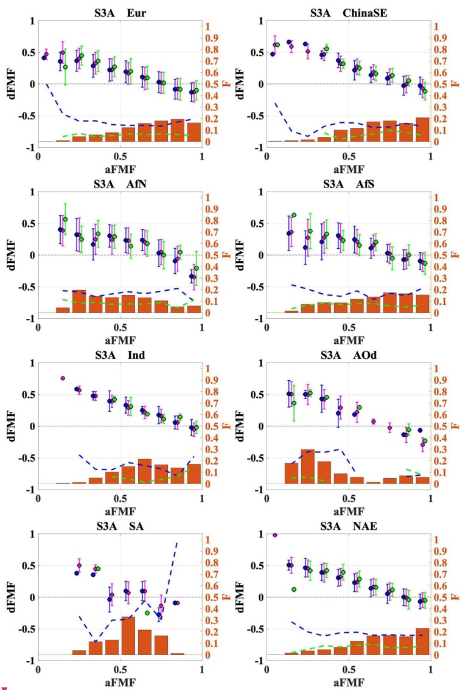

Figure 22: Regional (for Eur, ChinaSE, AfN, AfS, Ind, AOd, SA, NAE) difference (dFMF) between syFMF and aFMF for selected aFMF bins: median bias (circles) and bias standard deviation (error bars) for all AOD types (purple), aerosol fine-dominated AOD (blue) and coarse-dominated AOD (green). The fraction (F) of points in each bin from the total number of matchups is represented by orange bars. The fraction of fine-dominated matchups in each bin is shown as orange dashed-line. Results for other regions are in the Supplement (Figure S 11).

10.4 Ångström exponent

The Ångström exponent, AE, is often used as a qualitative indicator of aerosol particle size. Synergy AE (syAE) is calculated in the spectral interval 550-865 nm, while AERONET AE (aAE) is provided for 500-870 nm. The difference between $AE_{550-865}$ and $AE_{500-870}$ depends on the aerosol type and may be as high as 5-10% of AE (personal estimations). This difference must be considered for the interpretation of the evaluation results.

Scatter plots between $syAE_{550-865}$ and $aAE_{500-870}$ for S3A for all matchups and different groups of matchups are shown in Figure 23, corresponding validation statistics are shown in Table S5, Supplement. Two "clouds" of satellite/AERONET AE matchups are clearly observed. The first cloud is in the aAE interval of [1, 1.6] and syAE around 1.2. In that interval, the cloud of pixels

Deleted:

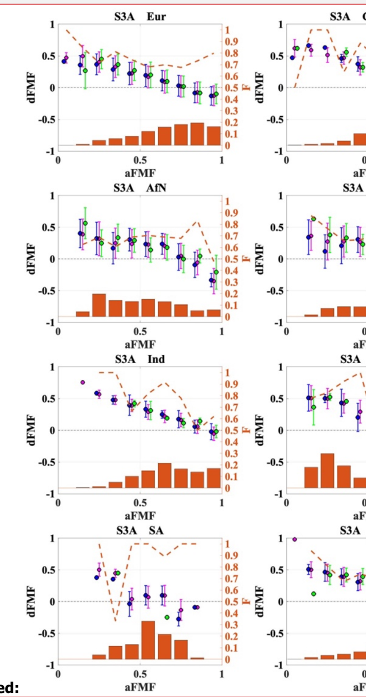

Deleted: and

Deleted: -

is located around the 1:1 line, which means that the agreement between syAE and aAE is quite good. Dual matchups contribute most to this "cloud". The second "cloud", formed mostly from the singleN and singleO groups of matchups, is in the aAE interval of [1.4, 1.9] and syAE around 2. In that interval, syAE is overestimated by 0.3-0.6.

For 40% of the matchups with AERONET in the NH, and for 60% of the matchups in the SH, which fit into the aAE interval of [1, 1.8], an offset between syAE and aAE is within ±0.25. General overestimation of low (<0.5) syAE and underestimation of high (>1.8) syAE is resulting in high (0.94, globally) overall bias.

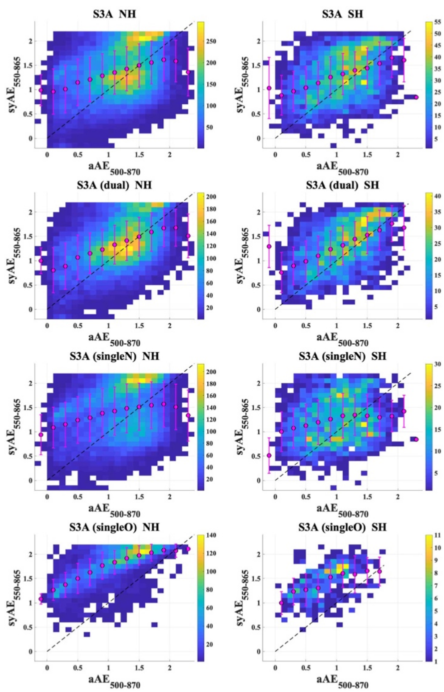

Figure 23: Scatter plots between $syAE_{550-865}$ and $aAE_{500-870}$ for S3A for the NH and SH (panels left and right, respectively) for different groups of products (top-down: all, dual, singleN and singleO).

For the whole global product, correlation coefficients between $syAE_{550-865}$ and $aAE_{500-870}$ are quite low, 0.35/0.34, rms is high, 0.57/0.58 for S3A/S3B, respectively. Validation statistics are slightly better for the dual product. The singleO product shows better correlation, but worse rms and std. Validation statistics are better in the NH for all matchups and the dual product. For the single view groups (singleN and singleO), no difference in validation results was revealed between the NH and SH.

Regional analysis (Figure 24, Table S6) reveals considerable differences in syAE evaluation results for regions with different surface type and aerosol properties. Footprints for the frequency of matchups at certain AE ranges (density value on the scatter plot) follow the "cloudy" shape in regional scatter density plots. Location of the "clouds" along x-axis (aAE) is specified by prevailing aerosol types in those regions. The "cloudy" shape of the footprint often ruins validation statistics, which should be interpreted with consideration of the matchup's footprint, Figure 24.

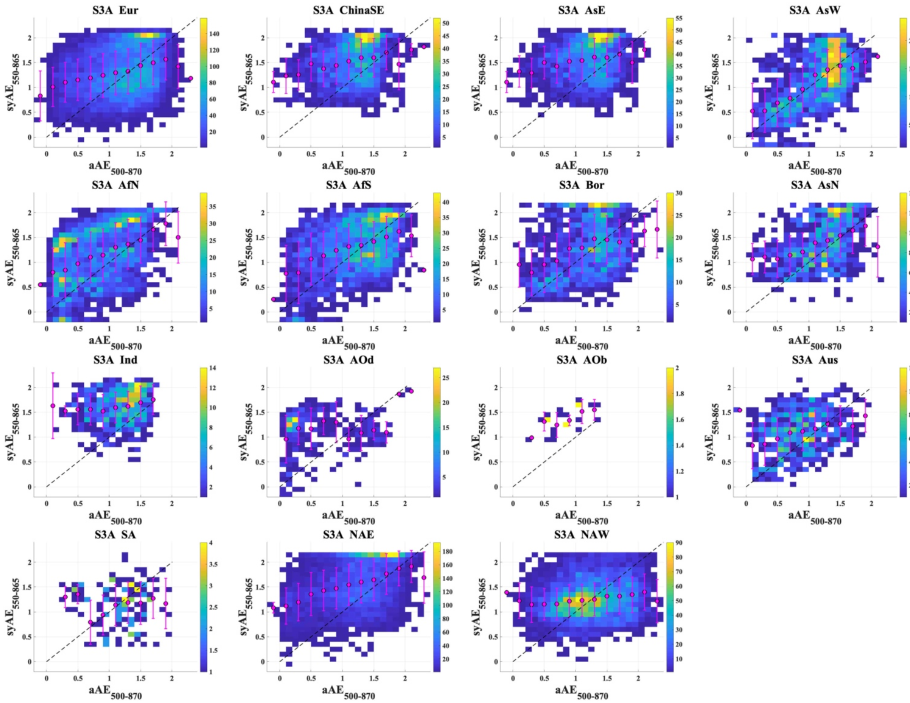

Figure 24: Regional scatter density plots between $syAE_{550-865}$ and $aAE_{500-870}$. Regions are defined in Figure 6.

syAE is often overestimated in the aAE range [1.3, 1.7], except for AsW, where the fraction of "good" (close to the 1:1 line) pixels is as high as fraction of overestimated syAOD. In AfN, low AE, which is typical for that region characterized by a high

Deleted: **Table 6: Validation statistics (number of points, N; correlation coefficient, R; root mean square, rms; standard deviation, σ; bias and slope defined with linear regression applied to all available matchups) for S3A and S3B $syAE_{550-865}$ for the globe, NH and SH for the whole period for all matchups and for three groups of matchups, defined with the processor applied.**
Group ... [4]

Deleted: Figure 24

Deleted: (, Supplement),

Deleted: Figure 24

Deleted: **Figure 6**

Deleted: Over land,

Deleted: of

Deleted: -

fraction of dust particles, is often highly overestimated. Dense cloud of "good" matchups is located near the 1:1 line in NAW. However, R (Table S6 in the Supplement) is low in that region, because, as mentioned above, the shape of the "good" pixels has a shape of a cloud and statistics are defined by outliers which are distributed evenly in all directions from the "cloud". In oceanic regions with possible transport of dust aerosols, syAE is often underestimated. The low number of matchups in AOb region (N = 22) doesn't allow making a solid conclusion on the syAE quality in this region.

11 Validation over ocean

Being performed on-board ships, MAN AOD measurements are irregular. S3A and S3B collocations with MAN for the period 01.2020-09.2021 are shown in Figure 25. Altogether, 105 matchups have been found for S3A and 95 matchups for S3B. Note, that about half of the collocations are observed near coastal zones. Since the number of validation points is low, we show in Figure 26 scatter plots and validation statistics for both S3A and S3B.

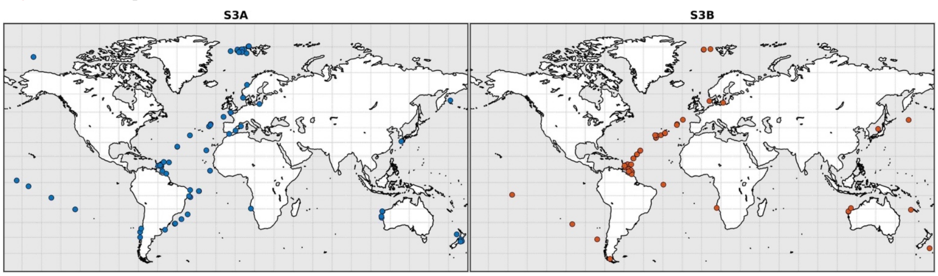

Figure 25: Collocations of S3A (left) and S3B (right) with MAN, 01.2020-09.2021

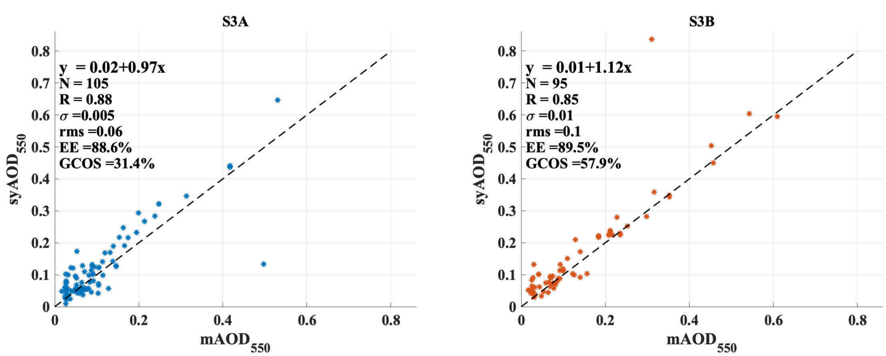

Figure 26: Scatter plots between S3A and S3B syAOD and MAN AOD (mAOD) with validation statistics.

Deleted: Location of the smaller "cloud" of pixels near the 1:1 line proves a good quality of syAE.

Deleted: Regional validation statistics for syAE (number of collocations per area N, R, rms, bias, slope) are summarised in. Rms is above 0.5 for all areas, except AsW. syAE bias is 0.35 in AsW, 0.7-1.0 on Eur, Bor, AsN, Aus, Afn, AfS and above 1.0 in the other regions. Slope is 0.72 in AsW, 0.4-0.5 in Bor, AsN, AfN, AfS and below 0.4 in the other regions.
Combination of the results shown in Figure 23 and summarised in Table 7, prove, in general, good quality of syAE, though R is often low. Positive syAE bias is clearly seen in AfN region for all aAE ranges and in the neighbouring AOd region for low aAE.
Table 7: For S3A, $syAE_{550-865}$ validation statistics: number of points, N; correlation coefficient, R; root mean square, rms; standard deviation, σ; bias and slope defined with linear regression applied to all available matchups.
Region ... [5]

Results for both instruments confirm a good performance of the retrieval algorithm over ocean. For S3A/S3B, correlation coefficients are 0.88/0.85, fractions of pixels in the EE are 88.6/89.5 %. An offset with MAN AOD (mAOD) is slightly higher for S3A (0.02/0.01), while rms is slightly higher for S3B (0.06/0.1).

One value from each product, S3A and S3B, can be considered as a clear outlier: S3A over the Baltic is underestimated, S3B over the Caribbean Sea is overestimated. The removal of these outliers from the validation exercise improves validation statistics: correlation increases to 0.95/0.97, rms decreases to 0.04/0.03, fractions of pixels in the EE increases to 89.4/92,4 % for S3A/S3B, respectively.

12 SY_2 AOD spatial performance relative to MODIS Terra DT&DB AOD product

12.1 Methods

The coverage of ground-based reference data is limited. To better evaluate a spatial distribution of the satellite retrieved AOD, the inter-comparison with other satellite products is necessary. The satellite product chosen as a "reference" must fulfil several criteria, e.g.:

(i) overpass time as close as possible to Sentinel-3 to avoid possible different aerosol and cloud conditions;

(ii) wider swath (for the reference product), which allows considering most of the pixels from the tested product in the analysis;

(iii) similar resolution, which allows pixel-to-pixel intercomparison.

Considering these criteria, the MODIS Terra DT&DB AOD product has been chosen as a reference for evaluation of the SY_2 AOD_{550} product.

MODIS Terra DT&DB AOD product fulfils two out of three criteria mentioned above:

(i) The Sentinel-3 orbit is a near-polar sun-synchronous orbit with a descending node equatorial crossing at 10:00 am Mean Local Solar time. The MODIS Terra satellite is crossing the equator on descending passes at 10:30 -10:45 AM.

(ii) SLSTR dual view swath centred on the sub-satellite track is 740 km wide, with a single view swath width of 1470 km. OLCI instrument covers a swath width of 1,270 km. MODIS Terra has a viewing swath width of 2,330 km.

The (iii) criteria is not fulfilled since MODIS and SY AOD products are provided at different resolutions. The resolution of the SY_2 product is 4.5x4.5 km^2, while the MODIS AOD daily product is available at 3km, 10km and 1° resolution, MODIS monthly product is available at 1° resolution. Thus, to fulfil the third criterion, we re-grided daily SY_2_AOD product to 1° resolution for an area of interest (AOI) and calculated monthly aggregates. One degree grid resolution was chosen to mitigate collocation uncertainties, smooth the data and minimise the processing time.

Two different approaches exist for evaluation and inter-comparison of satellite monthly AOD. For algorithm performance inter-comparison, only the spatio-temporally collocated pixels from the two products were considered (used in monthly aggregates). For climate studies (for, e.g., model evaluation, trend analysis),, where existing monthly products are utilized, an inter-comparison should be performed for the products built on all points available for each instrument, respectively.

Deleted: The

Deleted: is considered from two points of view

Deleted: when

Deleted: (for, e.g., model evaluation, trend analysis), SY_2 and MODIS Terra AOD products were inter-compared over the area shown in Figure 27 and Figure 28. To evaluate and inter-compare AOD products (and thus algorithm performance) in different environments (e.g., surface type, aerosol type, aerosol loading), sub-regions shown in Figure 29 (top right) were chosen (see Table S7 for details).

12.2 Inter-comparison of daily AOD products

All pixels available in S3A SY_2_AOD and MODIS Terra L3 daily AOD550 products, collocated products and differences between collocated products are shown for a selected area of interest (AOI) for 26 February 2020 (Figure 27). Because of the wider swath, MODIS has larger coverage than S3A. Thus, when collocating two products for closer intercomparison, more pixels from the MODIS product are removed.

For the products containing all original pixels for each instrument respectively, the SY_2 AOD mean over the AOI is higher than MODIS Terra AOD (0.35/0.21 for S3A/ MODIS, respectively). Mean AOD over land and over ocean are also higher for S3A. For collocated products, mean (over the AOI) AOD for S3A and MODIS, as well as AOD over ocean come very close to each other. However, SY_2 FMF (syFMF) over ocean (Figure 28) is lower than MODIS FMF (modFMF). Also, regional differences related mainly to possible dust overflow over Atlantic, exists. MODIS provides higher AOD over the dust plume. Lower modAOD on the west of the plume may be explained by the offset between MODIS Terra and S3A overpass time. Over land, mean AOD is slightly lower for S3A for collocated pixels. modFMF over bright surface (Sahara) is missing; over other regions the difference between syFMF and modFMF is lower compared to ocean.

For the chosen day, for S3A, a sharp transition between AOD retrieved over land and ocean at the west coast of Africa is revealed. This feature is clearly seen in the S3A and MODIS AOD difference plot. This can be explained by the land/surface gradient in the syFMF (Figure 28). The large AOD gradient in S3A data is observed over Nigeria; the inconsistency with MODIS data reaches above ±0.5 AOD in this area. MODIS FMF is not provided in this area.

Deleted: Figure 27

Deleted: inter-compare

Deleted: Figure 29

Deleted: S2

Formatted: Font: 10 pt, Not Bold

Deleted: th of

Deleted: Figure 27

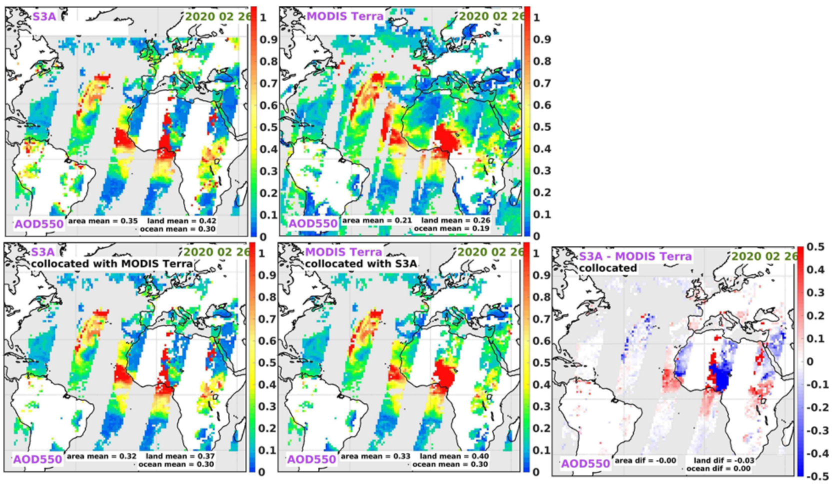

Figure 27: For 26 February 2020, upper panel: All pixels available in S3A syAOD_{550} (left), MODIS modAOD_{550} (middle) products. Lower panel: Pixels existing in both products (collocated products), syAOD_{550} (left), modAOD_{550} (middle) and difference between syAOD_{550} and modAOD_{550} (right). For each sub-plot, statistics (mean AOD for the whole area and separately for land and ocean) are shown.

Deleted: 2020-02-26

Deleted: U

Deleted: products,

Deleted: SY_2_

Deleted: Terra

Deleted: S3A

Deleted: SY_2_

Deleted: MODIS Terra

Deleted: S3A SY_2_AOD and MODIS Terra AOD

Deleted: for AOD_{550}

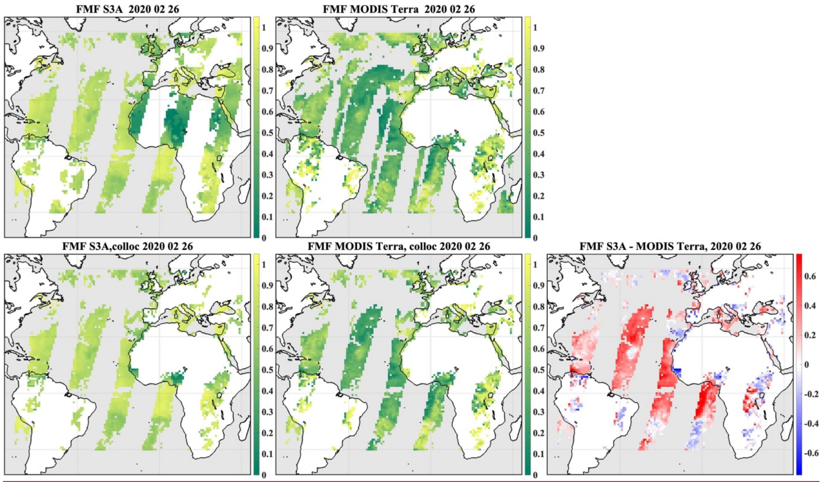

Figure 28: Same as Figure 27, syFMF, modFMF and difference between syFMF and modFMF

For the whole year 2020, S3A SY_2 and MODIS AOD$_{550}$ pixel-level inter-comparisons of 1°x 1° daily products for chosen sub-regions are shown as density scatter plots in Figure 29.

In Europe region, which includes parts of Eastern and Southern Europe and Middle East, AOD is low (<0.4) in both products, in general. However, several outliers are observed in SY_2 product (SY_2 AOD is in the range 1-4, while MODIS AOD is below 0.5). A possible reason for disagreement can be that SY_2 AOD was retrieved in cloud edge, while MODIS has been retrieving AOD in clear sky condition (given ca 30 min difference between overpasses). If this is true, SY_2 cloud screening should be improved to better distinguish between aerosol and clouds in cloud edge areas. The outlier cases should be studied separately to better understand a reason for disagreement.

In the desert area the disagreement between the two products is most significant. For MODIS AOD in the range 0-0.8 most of the SY_2 pixels have AOD<0.2, while there are also a considerable number of SY_2 pixels with AOD in the range 1-4. For MODIS AOD above 0.8, SY_2 AOD is often low, which is confirmed with averaged over MODIS AOD bins results (magenta dots in Figure 29). The high surface reflectance typical to this area is challenging for aerosol retrieval. The large variance observed in the AOD comparison indicates that a more detailed inter-comparison including the surface reflectance values retrieved by each algorithm should be performed. Over clean ocean and ocean+dust sub-regions, an agreement between SY_2 and MODIS AOD is quite good for modAOD<1 and modAOD<1.8, respectively; for higher AOD , syAOD is lower than MODIS AOD.

Deleted: Figure 29
Formatted: Font: 10 pt, Not Bold
Deleted: Figure 29
Formatted: Font: 10 pt, Not Bold
Deleted: though SY_2
Deleted: slightly
Deleted: when
Deleted: is above 0.8 and above 1.2, respectively

In coast+dust area (over which biomass burning aerosols can be transported occasionally), AOD averaged over bins are biased slightly positive for AOD<1.2, which results from SY_2 positive outliers, while for AOD>1.2 SY_2 AOD is often much lower than MODIS AOD, thus binned averaged AOD is biased negative.

The footprints for SY_2 and MODIS AOD look similar in the two areas with seasonal contribution of biomass burning aerosols (Africa,BB and S.America,BB). An agreement between SY_2 and MODIS is good for MODIS AOD below 1.2. Above that threshold, SY_2 AOD is on average lower.

Overall, the majority of data is in the low AOD range, where agreement is decent (with SY_2 slightly high biased), but at higher AOD there is much more variance (partly due to the scarcity of data), and in general a slight low-bias for SY_2.

Seasonal comparison is shown in Figure S13, supplement. Annual and seasonal statistics for SY_2 and MODIS Terra for all daily pixel AOD inter-comparison are summarised in the supplement (Table S8).

Deleted: S12

Deleted: 2, Table S3

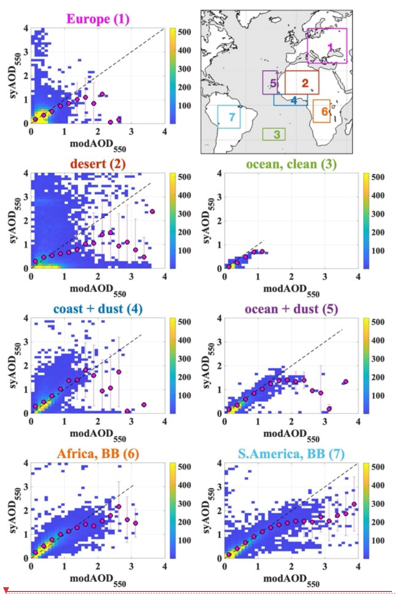

Deleted:

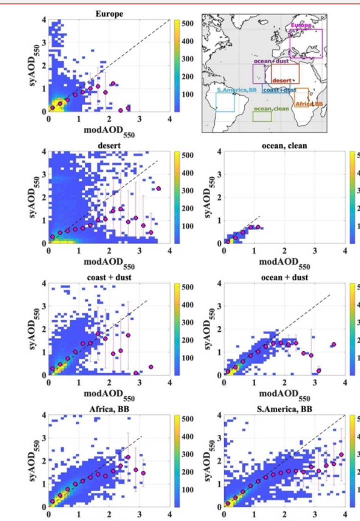

Figure 29: Density scatter plots for MODIS Terra and S3A SY_2_AOD L3 daily collocated products for 2020 for the sub-regions shown in the top right corner. Statistics are summarised in the Supplement (Table S9).

Deleted: 1, Table S2

12.3 Spatial inter-comparison of seasonal and annual S3A and MODIS Terra AOD products

Deleted: monthly,

Two types of monthly datasets have been created from SY_2_AOD and MODIS Terra daily data to study the differences at monthly/seasonal/annual (MSA) level.

In the first monthly dataset, all pixels available in SY_2_AOD and MODIS Terra daily products have been used to build a monthly aggregate, respectively for each instrument. Inter-comparison of these 'all pixels' monthly aggregates (which are similar to the official monthly products provided for users) is important because it will help in, e.g., understanding the difference in climate data records which are built from the provided monthly AOD products which include all available data.

A second monthly dataset, 'collocated' product, has been aggregated using only collocated daily pixels. Inter-comparison of 'collocated' monthly aggregates shows the difference in monthly AOD based on differences in retrieval approaches.

Deleted: instruments and

Annual AOD from 'all pixels' and 'collocated' monthly datasets for SY_2_AOD and MODIS Terra, respectively, and the corresponding differences are shown in Figure 30. Seasonal plots for collocated aggregates and difference between them are shown in Figure 31. Statistics for difference plots (area/land/ocean means) have been calculated from pixel-to-pixel difference, but not as difference between the AOD averaged over AOI, land and ocean.

Differences between SY_2_AOD and MODIS Terra MSA AOD exist in both 'all pixels' and 'collocated' datasets. For both datasets, SY_2 AOD averaged over AOI is higher for the whole area, as well as for land and ocean. The difference is smoother for 'all pixels' datasets. Even though difference plots show that regional offset between two datasets is often within GCOS requirements of AOD quality (0.03) over ocean (SY_2 AOD is in general lower) and whole AOI, difference in AOD over land is often higher (up to 0.11 as averaged over AOI in DJF, 'all pixels' dataset).

Deleted: (annual: Figure 29; seasonal: Figure 30 and Figure S6; monthly results are not shown)

Regional differences in seasonal AOD from the 'collocated' dataset are considerably higher (Figure 31). For all land sub-regions (except for 'desert', JJA), S3A AOD is higher than MODIS AOD. The offset is highest for 'coast+dust' region in DJF and for 'Africa,BB' region in SON (0.18 and 0.15, respectively). General tendency of decreasing offset towards JJA months has been observed. However, though the offset is often high, time series for both products are within an overlap (grey area) of the standard deviations for individual products. Highest negative offset (between 0.05 and 0.1) is observed in JJA in the 'desert' region. Regional differences in seasonal AOD from the 'all pixels' dataset are less scattered (Figure S6, Supplement).

For the open ocean regions ('ocean, clean' and 'ocean+dust'), S3A AOD is in general lower than MODIS AOD for all MSA; the exceptions are January and February in 'ocean+dust' region (Figures not shown). In the annual scale, the offset between S3A and MODIS AOD is -0.02 for 'ocean+dust' and -0.03 for 'ocean, clean'. AOD in 'collocated' dataset is higher compared to 'all pixels' dataset for both S3A SY_2 and MODIS Terra. Comparing with 'all pixels', 'collocated' SY_2 AOD product looks less smooth over Northern Africa in DJF and MAM.

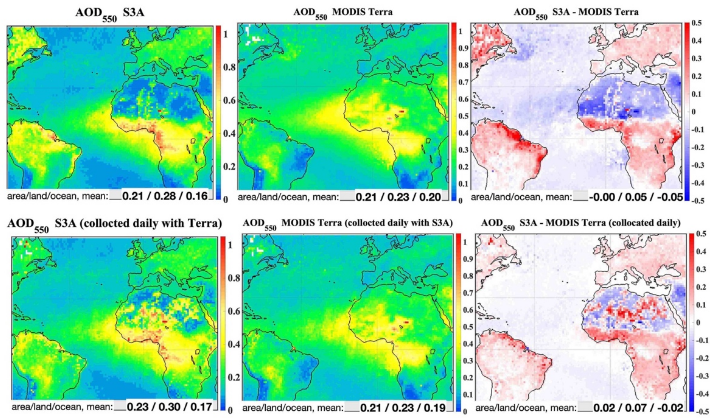

Figure 30: For year 2020, annual S3A SY_2_AOD (left panel), MODIS Terra (middle panel) AOD and difference in between S3A and MODIS Terra (right panel) AOD. Annual means are calculated from monthly aggregates combined from all data available in each product (upper panel) and pixels of collocated daily AOD (lower panel). AOD mean and difference between SY_2 and MODIS AOD for the whole area, as well as separately for land and ocean, are shown on the maps.

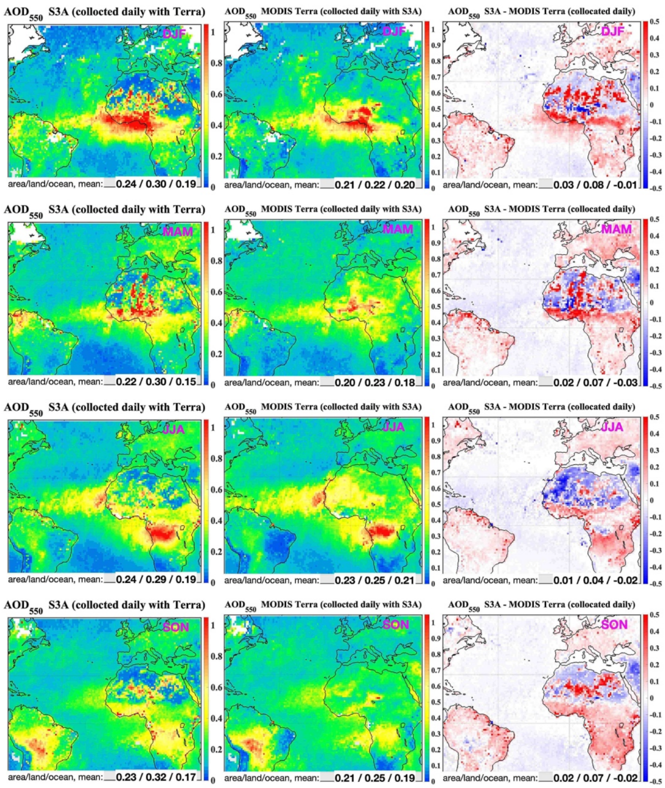

Figure 31: Seasonal (top down: DJF, MAM, JJA, SON) S3A (left panel), MODIS Terra (middle panel) AOD_{550} and difference in AOD_{550} between S3A and MODIS Terra (right panel). From monthly aggregates created from collocated daily S3A and MODIS Terra AOD products.

13 Conclusions and recommendations for future evolution

We have presented the first validation of a new SYNERGY global aerosol product, derived from the data from the OLCI and SLSTR sensors onboard the Sentinel-3A and -3B satellites. Combined, the two satellites provide close to daily global coverage and provide aerosol measurements with a latency of 2-3 days. In this study we have compared the aerosol product with ground-based photometer data from four networks: AERONET, SKYNET, SURFRAD, and MAN, and with MODIS combined Dark

Target and Deep Blue algorithms. The aim of this study was to provide global characterisation of the current aerosol retrieval, and to guide future algorithm development.

Over ocean, the performance of SYNERGY retrieved AOD is good and consistent with reference MAN dataset (rms ~0.05), although the MAN validation has a limited set of higher AOD examples. Against MODIS, agreement is good, although SYNERGY AOD shows lower values at high AOD (>1.5) in dust regions, potentially indicating cloud screening improvement needed to correctly detect high dust levels.

Over land, overall performance has a much higher rms error, approximately 0.25 when compared to AERONET. Overall AERONET correlation is ~0.6. Reduced performance over land is expected since the surface reflectance and angular distribution of scattering are higher, and they are more difficult to treat over land than over ocean. However, the results show that these statistics are affected by a large number of outliers. Inspection of these outliers and patterns of disagreement with MODIS indicate possible reasons and targets for future algorithm evolution. The main causes are (i) poor screening of snow/ice covered surfaces, (ii) inadequate cloud screening in some regions. For example, in tropical forest areas, care needs to be taken to fully exclude any pixels containing clouds, including sub-pixel clouds in either nadir or oblique view. In addition, removal of cloud edge pixels (cloud free pixels next to cloud masked pixels) should be considered. Bright desert surfaces also have less stable retrieval, with land/ocean contrast suggesting high values in dust plumes are underestimated over land. Further uncertainty is introduced by an error in a priori estimates of aerosol properties not retrieved, principally single scattering albedo (SSA).

It is clear that retrievals using dual view give higher quality, making use of more information to allow less reliance on surface spectral assumptions. Retrieval over land surface in the Northern Hemisphere shows generally higher retrieval error, including regions of boreal forest where we would expect higher quality retrieval due to the low surface signal. In some cases, this will be due to weak masking of snow and ice cover, and the presence of retrievals made at high solar zenith angles (over 70°) often excluded in other aerosol datasets. In addition, since the land retrieval relies on use of the oblique SLSTR view we expect to see higher quality retrievals in the SH compared to NH. This is due mainly to sampling of backscattered light by the SLSTR oblique view in NH, where aerosol has a weak signal, and the surface signal is higher, while in SH the geometry is reversed. Over ocean this is not the case, as the retrieval is not reliant on the oblique view, and indeed the geometry results in less sunglint in NH ocean.

The retrieval of Angström exponent, related to aerosol size distribution, shows spatial correlation with expected sources but generally overestimates AE for cases where AERONET Angström is low, resulting in overall high bias. This is dependent on the retrieval of fine mode fraction in the algorithm, which needs to be investigated further and improved. Evaluation of the per-retrieval uncertainty indicated good correlation with measured error distributions, with overprediction of expected error in dual view case, and underprediction in single view case. Evaluation of the uncertainty propagation is difficult in the presence of outliers which do not fit the algorithm assumptions, where we see a tail of higher errors, for example related to undetected cloud in the input data.

Deleted: Angstrom

Deleted: Angstrom

Author contribution

CH, LS and SD created the original research framework and provided research direction. MD, CH established a data base. LS developed a validation strategy, wrote the software and performed the analysis. PK co-wrote the software. LS, TV, PN, CH, SS and SD co-wrote the manuscript.

Competing interests

The contact author has declared that neither they nor their co-author has any competing interests.

Funding

This work has been performed in the frame of the LAW project under the European Space Agency Contract 4000129877/20/I-BG.

Data access

SY_2_AOD product: https://scihub.copernicus.eu/dhus/#/home , last access 13 March 2022

Deleted: .03.

SY_2_AOD product validation matchups: https://law.acri-st.fr/home, last access 10 January 2022

Deleted: .01.

References

Arbor, A., Briley, L., Dougherty, R., Wells, K., Hercula, T., Notaro, M., Rood, R., Andresen, J., Marsik, F., Prosperi, A., Jorns, J., Channell, K., Hutchinson, S., Kemp, C., and Gates, O.: A Practitioner's Guide to Climate Model Scenarios. Great Lakes Integrated Sciences and Assessments (GLISA). https://glisa.umich.edu/wp-content/uploads/2021/03/A_Practitioners_Guide_to_Climate_Model_Scenarios.pdf, 2021.

Augustine, J. A., Hodges, G. B., Cornwall, C. R., Michalsky, J. J., and Medina, C. I.: An update on SURFRAD - The GCOS Surface Radiation budget network for the continental United States. Atmos. and Oceanic Techol., 22(10), 1460-1472, doi:10.1175/JTECH1806.1., 2005.

Bergquist, P., and Warshaw, C.: Does global warming increase public concern about climate change? J. Polit. 81, 686–691, 2019.

Bevan, S.L., North, P.R.J., Los, S.O. and Grey, W.M.F.: A global dataset of atmospheric aerosol optical depth and surface reflectance from AATSR. Remote Sensing of Environment, 116, 119-210, 2012.

Borowitz, M.: Open space. The global effort for open access to environmental satellite data, Cambridge, MA, MIT Press, ISBN:9780262037181, 432 pp., 2018.

Chu, D. A., Kaufman, Y. J., Ichoku, C., Remer, L. A., Tanre, D., and Holben, B. N.: Validation of MODIS aerosol optical depth retrieval over land. Geophys. Res. Lett., 29, 8007, doi:10.1029/2001GL013205, 2002.

Committee on Earth Observation Satellites (CEOS); Coordination Group for Meteorological Satellites (CGMS). Space Agency Response to GCOS Implementation Plan–The Joint CEOS/CGMS Working Group on Climate (WGClimate). http://ceos.org/document_management/Working_Groups/WGClimate/Documents/Space%20Agency%20Response%20to%20GCOS%20IP%20v2.2.1.pdf, 2017.

Cox, C. and Munk, W.: Measurements of the roughness of the sea surface from photographs of the Sun's glitter. J. Opt. Soc. Am., 44, 838–850, 1954.

Davies, W. & North, P.: Synergistic angular and spectral estimation of aerosol properties using CHRIS/PROBA-1 and simulated Sentinel-3 data. Atm. Meas.Tech., 8(4), 1719-1731, 2015.

de Leeuw, G., Holzer-Popp, T., Bevan, S., Davies, W., Descloitres, J., Grainger, R.G., Griesfeller, J., Heckel, A., Kinne, S., Klüser, L., Kolmonen, P., Litvinov, P., Martynenko, D., North, P. J. R., Ovigneur, B., Pascal, N., Poulsen, C., Ramon, D., Schulz, M., Siddans, R., Sogacheva, L., Tanré, D., Thomas, G. E., Virtanen, T. H., von Hoyningen Huene, W., Vountas, M., and Pinnock, S.: Evaluation of seven European aerosol optical depth retrieval algorithms for climate analysis. Remote Sensing of Environment, 162, 295-315. 10.1016/j.rse.2013.04.023, 2015.

Dubovik, O., Schuster, G. L., Xu, F., Hu, Y., Bösch, H., Landgraf, J., and Li, Z.: Grand Challenges in Satellite Remote Sensing. Front. Remote Sens. 2:619818. doi: 10.3389/frsen.2021.619818, 2021.

Eck, T. F., Holben, B. N., Reid, J. S., Dubovik, O., Smirnov, A., O'Neill, N. T., Slutsker, I., and Kinne, S.: Wavelength dependence of the optical depth of biomass burning, urban, and desert dust aerosols, J. Geophys. Res., 104, 31,333–31,349, doi:10.1029/1999JD900923, 1999.

ESA Aerosol CCI portal, available at: https://climate.esa.int/en/projects/aerosol/key-documents/, last access: 25 February 2022.

Deleted: .02.

Estelles, V., Campanelli, M., Utrillas, M. P., Exposito, F., and Martinez-Lozano, J. A.: Comparison of AERONET and SKYRAD4.2 inversion products retrieved from a Cimel CE318 sunphotometer. Atmos. Meas. Tech., 5, 569-579, doi:10.5194/amt-5-569-2012, 2012.

Eyre, J. R., Bell, W., Cotton, J., English, S. J., Forsythe, M., Healy, S. B., and Pavelin, E. G.: Assimilation of satellite data in numerical weather prediction. Part II: Recent years. Quarterly Journal of the Royal Meteorological Society, 1-36, https://doi.org/10.1002/qj.4228, 2022.

GCOS, 2016, https://ane4bf-datap1.s3.eu-west-1.amazonaws.com/wmod8_gcos/s3fs-public/aerosols_ecv_factsheet_201905.pdf?Sv_8X3rsnl_rqNQVLEIg5gzig53zTHox, last access: 25 February 2022.

Deleted: .02.

Giles, D. M., Sinyuk, A., Sorokin, M. G., Schafer, J. S., Smirnov, A., Slutsker, I., Eck, T. F., Holben, B. N., Lewis, J. R., Campbell, J. R., Welton, E. J., Korkin, S. V., and Lyapustin, A. I.: Advancements in the Aerosol Robotic Network (AERONET) Version 3 database – automated near-real-time quality control algorithm with improved cloud screening for Sun photometer aerosol optical depth (AOD) measurements, Atmos. Meas. Tech., 12, 169-209, https://doi.org/10.5194/amt-12-169-2019, 2019.

Gliß, J., Mortier, A., Schulz, M., Andrews, E., Balkanski, Y., Bauer, S. E., Benedictow, A. M. K., Bian, H., Checa-Garcia, R., Chin, M., Ginoux, P., Griesfeller, J. J., Heckel, A., Kipling, Z., Kirkevåg, A., Kokkola, H., Laj, P., Le Sager, P., Lund, M. T., Lund Myhre, C., Matsui, H., Myhre, G., Neubauer, D., van Noije, T., North, P., Olivié, D. J. L., Rémy, S., Sogacheva, L., Takemura, T., Tsigaridis, K., and Tsyro, S. G.: AeroCom phase III multi-model evaluation of the aerosol life cycle and optical properties using ground- and space-based remote sensing as well as surface in situ observations, Atmos. Chem. Phys., 21, 87–128, https://doi.org/10.5194/acp-21-87-2021, 2021.

Harris, R. and Baumann, I.: Open data policies and satellite Earth observation, Space Policy, Volume 32, pp. 44-53, ISSN 0265-9646, https://doi.org/10.1016/j.spacepol.2015.01.001, 2015.

Hashimoto, M., Nakajima, T., Dubovik, O., Campanelli, M., Che, H., Khatri, P., Takamura, T., and Pandithurai, G.: Development of a new data-processing method for SKYNET sky radiometer observations, Atmos. Meas. Tech., 5, 2723-2737, 2012.

Hoffmann, R., Muttarak, R., Peisker, J. and Stanig, P.: Climate change experiences raise environmental concerns and promote Green voting. Nat. Clim. Chang. 12, 148–155, https://doi.org/10.1038/s41558-021-01263-8, 2022.

Holben, B. N., Eck, T. F., Slutsker, I., Tanré, D., Buis, J. P., Setzer, A., Vermote, E., Reagan, J.A., Kaufman, Y., Nakajima, T., Lavenu, F., Jankowiak, I., and Smirnov, A.: AERONET — A federated instrument network and data archive for aerosol characterization, Remote Sens. of Env., 66, 1–16, 1998.

Holzer-Popp, T., de Leeuw, G., Griesfeller, J., Martynenko, D., Klüser, L., Bevan, S., Davies, W., Ducos, F., Deuzé, J. L., Graigner, R. G., Heckel, A., von Hoyningen-Hüne, W., Kolmonen, P., Litvinov, P., North, P., Poulsen, C. A., Ramon, D., Siddans, R., Sogacheva, L., Tanre, D., Thomas, G. E., Vountas, M., Descloitres, J., Griesfeller, J., Kinne, S., Schulz, M., and Pinnock, S.: Aerosol retrieval experiments in the ESA Aerosol_cci project, Atmos. Meas. Tech., 6, 1919–1957, https://doi.org/10.5194/amt-6-1919-2013, 2013.

Ichoku, C., Chu, D. A., Chu, S., Kaufman, Y. J., Remer, L. A., Tanré, D., Slutsker, I., and Holben, B. N.: A spatio-temporal approach for global validation and analysis of MODIS aerosol products, Geophys. Res. Lett., 29(12), 8006, doi:10.1029/2001GL013206, 2002.

Julien,Y., and Sobrino, J.A.: NOAA-AVHRR Orbital Drift Correction: Validating Methods Using MSG-SEVIRI Data as a Benchmark Dataset. Remote Sens.,13, 925. https://doi.org/ 10.3390/rs13050925, 2021.

Khaki, M., Hendricks Franssen, H.J., and Han, S.C.: Multi-mission satellite remote sensing data for improving land hydrological models via data assimilation. Sci. Rep. 10, 18791, https://doi.org/10.1038/s41598-020-75710-5, 2020.

Kinne, S., D. O'Donnel, P. Stier, S. Kloster, K. Zhang, H. Schmidt, S. Rast, M. Giorgetta, T. F. Eck, and B. Stevens (2013): MAC-v1: A new global aerosol climatology for climate studies, J. Adv. Model. Earth Syst., 5, 704–740, doi:10.1002/james.20035.

Koepke, P.: Effective Reflectance of Oceanic Whitecaps, Applied Optics, 23(11), 1816-1824, 1984.

Leiserowitz, A., Maibach, E., Rosenthal, S., Kotcher, J., Bergquist, P., Ballew, M., Goldberg, M., Gustafson, A., and Wang, X.: Climate Change in the American Mind: April 2020. Yale University and George Mason University. New Haven, CT: Yale Program on Climate Change Communication. (https://climatecommunication.yale.edu/publications/climate-change-in-the-american-mind-april-2020/, last access 14 February 2022).

Deleted: .02.

Levy, R. C., Mattoo, S., Munchak, L. A., Remer, L. A., Sayer, A. M., Patadia, F., and Hsu, N. C.: The Collection 6 MODIS aerosol products over land and ocean, Atmos. Meas. Tech., 6, 2989–3034, https://doi.org/10.5194/amt-6-2989-2013, 2013.

Loew, A., Bell, W., Brocca, L., Bulgin, C. E., Burdanowitz, J., Calbet, X., Donner, R. V., Ghent, D., Gruber, A., Kaminski, T., Kinzel, J., Klepp, C., Lambert, J.-C., Schaepman-Strub, G., Schröder, M., and Verhoelst, T.: Validation practices for satellite-based Earth observation data across communities, Rev. Geophys., 55, 779–817, https://doi.org/10.1002/2017RG000562, 2017.

Meehl, G.A., Stocker, T. F., Collins, W. D., Friedlingstein, P., Gaye, A. T., Gregory, J. M., Kitoh, A., Knutti, R., Murphy, J. M., Noda, A., Raper, S. C. B., Watterson, I. G., Weaver, A. J., and Zhao, Z.-C.: Global Climate Projections. In: Climate Change

2007: The Physical Science Basis. Contribution of Working Group I to the Fourth Assessment Report of the Intergovernmental Panel on Climate Change. Cambridge University Press, Cambridge, U.K., 747-846, https://www.ipcc.ch/report/ar4/wg1/ (last access 13 March 2022), 2007.

Deleted: .03.

Monahan, E.C. and O'Muircheartaigh, I.: Optimal power-law description of oceanic whitecap dependence on wind speed, Journal of Physical Oceanography, 10(12), 2094–2099, 1980.

Morel, A.: Optical modeling of the upper ocean in relation to its biogenous matter content (case I waters), J. Geoph. Res., 93(C9), 10749-10768, 1988.

Morys, M., Mims III, F. M., Hagerup, S., Anderson, E., Baker, A., Kia, J., and Walkup, T.: Design, calibration, and performance of MICROTOPS II handheld ozone S. monitor and Sun photometer, J. Geophys. Res., 106, 14,573–14,582, doi:10.1029/2001JD900103, 2001.

North, P. R. J.: Estimation of aerosol opacity and land surface bidirectional reflectance from ATSR-2 dual-angle imagery: Operational method and validation, J. Geophys. Res., 107, doi:10.1029/2000JD000,207, 2002.

North, P.R.J., Brockmann, C., Fischer, J., Gomez-Chova, L., Grey, W., Heckle A., Moreno, J., Preusker, R. and Regner, P.: MERIS/AATSR synergy algorithms for cloud screening, aerosol retrieval and atmospheric correction. In Proc. 2nd MERIS/AATSR User Workshop, ESRIN, Frascati, 22- 26 September 2008. (CD-ROM), ESA SP-666, ESA Publications Division, European Space Agency, Noordwijk, The Netherlands, 2008.

North, P., and Heckel, A.: AOD-SYN Algorithm Theoretical Basis Document, V 1.12, S3-L2-AOD-SYN-ATBD, https://sentinels.copernicus.eu/documents/247904/0/SYN_L2-3_ATBD.pdf/8dfd9043-5881-4b38-aae5-86fb9034a94d, 2019.

Olbrich, P.: Open space: The global effort for open access to environmental satellite data. Astropolitics*,* 16, 230 – 236, 2018.

Popp, T. , de Leeuw, G.; Bingen, C.; Brühl, C.; Capelle, V.; Chedin, A.; Clarisse, L.; Dubovik, O.; Grainger, R.; Griesfeller, J.; Heckel, A.; Kinne, S.; Klüser, L.; Kosmale, M.; Kolmonen, P.; Lelli, L.; Litvinov, P.; Mei, L.; North, P.; Pinnock, S.; Povey, A.; Robert, C.; Schulz, M.; Sogacheva, L.; Stebel, K.; Stein Zweers, D.; Thomas, G.; Tilstra, L.G.; Vandenbussche, S.; Veefkind, P.; Vountas, M.; Xue, Y.: Development, Production and Evaluation of Aerosol Climate Data Records from European Satellite Observations (Aerosol_cci). Remote Sensing, 8(5), 421 doi:10.3390/rs8050421, 2016.

Remer, L. A., Kaufman, Y. J., Tanré, D., Mattoo, S., Chu, D. A., Martins, J. V., Li, R.-R., Ichoku, C., Levy, R. C., Kleidman, R. G., Eck, T. F., Vermote, E., and Holben, B. N.: The MODIS Aerosol Algorithm, Products, and Validation, J. Atmos. Sci., 62, 947–973, 2005.

Remer, L. A., Mattoo, S., Levy, R. C., and Munchak, L. A.: MODIS 3 km aerosol product: algorithm and global perspective, Atmos. Meas. Tech., 6, 1829–1844, https://doi.org/10.5194/amt-6-1829-2013, 2013.

Sayer, A. M., Hsu, N. C., Bettenhausen, C., Ahmad, Z., Holben, B. N., Smirnov, A., Thomas, G. E., and Zhang, J.: SeaWiFS Ocean Aerosol Retrieval (SOAR): Algorithm, validation, and comparison with other data sets, J. Geophys. Res., 117, D03206, https://doi.org/10.1029/2011JD016599, 2012a.

Sayer, A. M., Hsu, N. C., Bettenhausen, C., Jeong, M.-J., Holben, B. N., and Zhang, J.: Global and regional evaluation of over-land spectral aerosol optical depth retrievals from SeaWiFS, Atmos. Meas. Tech., 5, 1761–1778, https://doi.org/10.5194/amt-5-1761-2012, 2012b.

Sayer, A. M., Hsu, N. C., Bettenhausen, C. and Jeong, M.-J.: Validation and uncertainty estimates for MODIS Collection 6 “Deep Blue” aerosol data, J. Geophys. Res., 118, 7864– 7872, doi:10.1002/jgrd.50600., 2013.

Sayer, A. M., N. C. Hsu, J. Lee, W. V. Kim, O. Dubovik, S. T. Dutcher, D. Huang, P. Litvinov, A. Lyapustin, J. L. Tackett, and D. M. Winker: Validation of SOAR VIIRS over-water aerosol retrievals and context within the global satellite aerosol data record, J. Geophys. Res.-Atmos., 123, 13496–13526, https://doi.org/10.1029/2018JD029465, 2018.

Sayer, A. M., Hsu, N. C., Lee, J., Kim, W., and Dutcher, S.: Validation, stability, and consistency of MODIS Collection 6.1 and VIIRS Version 1 Deep Blue aerosol data over land, J. Geophys. Res.-Atmos., 124, 4658–4688, https://doi.org/10.1029/2018JD029598, 2019.

Sayer, A. M., Govaerts, Y., Kolmonen, P., Lipponen, A., Luffarelli, M., Mielonen, T., Patadia, F., Popp, T., Povey, A. C., Stebel, K., and Witek, M. L.: A review and framework for the evaluation of pixel-level uncertainty estimates in satellite aerosol remote sensing, Atmos. Meas. Tech., 13, 373–404, https://doi.org/10.5194/amt-13-373-2020, 2020a.

Shi, Y., Zhang, J., Reid, J. S., Hyer, E. J., and Hsu, N. C.: Critical evaluation of the MODIS Deep Blue aerosol optical depth product for data assimilation over North Africa, Atmos. Meas. Tech., 6, 949–969, https://doi.org/10.5194/amt-6-949-2013, 2013

Smirnov, A., B. N. Holben, I. Slutsker, D. M. Giles, C. R. McClain, T. F. Eck, S. M. Sakerin, A. Macke, P. Croot, G. Zibordi, P. K. Quinn, J. Sciare, S. Kinne, M. Harvey, T. J. Smyth, S. Piketh, T. Zielinski, A. Proshutinsky, J. I. Goes, N. B. Nelson, P. Larouche, V. F. Radionov, P. Goloub, K. Krishna Moorthy, R. Matarrese, E. J. Robertson, and F. Jourdin: Maritime Aerosol Network as a component of Aerosol Robotic Network, J. Geophys. Res., 114, D06204, doi:10.1029/2008JD011257, 2009.

Smirnov, A., Holben, B.N., Sakerin, S.M., Kabanov, D.M., Slutsker, I., Chin, M., Diehl, T.L., Remer, L.A., Kahn, R., Ignatov, A., Liu, L., Mishchenko, M., Eck, T.F., Kucsera, T.L., Giles, D. and Kopelevich, O.V.: Ship-Based Aerosol Optical Depth Measurements in the Atlantic Ocean: Comparison with Satellite Retrievals and Gocart Model. Geophysical Research Letters, 33, Article ID: L14817. https://doi.org/10.1029/2006GL026051, 2006.

Smirnov, A., Holben, B. N., Giles, D. M., Slutsker, I., O'Neill, N. T., Eck, T. F., Macke, A., Croot, P., Courcoux, Y., Sakerin, S. M., Smyth, T. J., Zielinski, T., Zibordi, G., Goes, J. I., Harvey, M. J., Quinn, P. K., Nelson, N. B., Radionov, V. F., Duarte, C. M., Losno, R., Sciare, J., Voss, K. J., Kinne, S., Nalli, N. R., Joseph, E., Krishna Moorthy, K., Covert, D. S., Gulev, S. K., Milinevsky, G., Larouche, P., Belanger, S., Horne, E., Chin, M., Remer, L. A., Kahn, R. A., Reid, J. S., Schulz, M., Heald, C. L., Zhang, J., Lapina, K., Kleidman, R. G., Griesfeller, J., Gaitley, B. J., Tan, Q., and Diehl, T. L.: Maritime aerosol network as a component of AERONET – first results and comparison with global aerosol models and satellite retrievals, Atmos. Meas. Tech., 4, 583–597, https://doi.org/10.5194/amt-4-583-2011, 2011.

Sogacheva, L., Kolmonen, P., Virtanen, T. H., Rodriguez, E., Saponaro, G., and de Leeuw, G.: Post-processing to remove residual clouds from aerosol optical depth retrieved using the Advanced Along Track Scanning Radiometer, Atmos. Meas. Tech., 10, 491–505, https://doi.org/10.5194/amt-10-491-2017, 2017.

Sogacheva, L., de Leeuw, G., Rodriguez, E., Kolmonen, P., Georgoulias, A. K., Alexandri, G., Kourtidis, K., Proestakis, E., Marinou, E., Amiridis, V., Xue, Y., and van der A, R. J.: Spatial and seasonal variations of aerosols over China from two decades of multi-satellite observations – Part 1: ATSR (1995–2011) and MODIS C6.1 (2000–2017), Atmos. Chem. Phys., 18, 11389-11407, https://doi.org/10.5194/acp-18-11389-2018, 2018a.

Sogacheva, L., Rodriguez, E., Kolmonen, P., Virtanen, T. H., Saponaro, G., de Leeuw, G., Georgoulias, A. K., Alexandri, G., Kourtidis, K., and van der A, R. J.: Spatial and seasonal variations of aerosols over China from two decades of multi-satellite observations – Part 2: AOD time series for 1995–2017 combined from ATSR ADV and MODIS C6.1 and AOD tendency estimations, Atmos. Chem. Phys., 18, 16631–16652, https://doi.org/10.5194/acp-18-16631-2018, 2018b.

Sogacheva, L., Popp, T., Sayer, A. M., Dubovik, O., Garay, M. J., Heckel, A., Hsu, N. C., Jethva, H., Kahn, R. A., Kolmonen, P., Kosmale, M., de Leeuw, G., Levy, R. C., Litvinov, P., Lyapustin, A., North, P., Torres, O., and Arola, A.: Merging regional and global aerosol optical depth records from major available satellite products, Atmos. Chem. Phys., 20, 2031–2056, https://doi.org/10.5194/acp-20-2031-2020, 2020.

Takamura, T., and Nakajima, T.: Overview of SKYNET and its activities, Opt. Pura Apl. 37, 3303-3308, 2004.

Wei, J., Li, Z. Q., Peng, Y. R., & Sun, L.: MODIS Collection 6.1 aerosol optical depth products over land and ocean: Validation and comparison. Atmospheric Environment, 201, 428– 440. https://doi.org/10.1016/j.atmosenv.2018.12.004, 2019.

Page 32: [1] Deleted **Sogacheva Larisa (FMI)** **14/07/2022 12:36:00**

Page 36: [2] Deleted **Sogacheva Larisa (FMI)** **14/07/2022 12:41:00**

Page 38: [3] Deleted **Sogacheva Larisa (FMI)** **14/07/2022 12:48:00**

Page 48: [4] Deleted **Sogacheva Larisa (FMI)** **14/07/2022 12:53:00**

Page 49: [5] Deleted **Sogacheva Larisa (FMI)** **20/07/2022 21:30:00**